Brief introduction to Basic Structures of Matter theory and derived atomic models

S. Sarg

Abstract. Our vision about the physical reality might be distorted if the currently adopted concept about vacuum is not correct. This may refer to processes in the micro world - beyond the limit of detection, and in the macro world - events of cosmological time scale. The thesis titled Basic Structures of Matter (BSM) presents a theory based on one alternative concept about the vacuum space that has not been studied in history of physics. The suggested concept provides a reference point allowing separation of space from time parameters in the analysis. This gives a possibility for theoretical study of complex physical phenomena in three dimensional space and unidirectional time scale with strongly observed principles of objective reality, causality and logical understanding. Analysing physical phenomena from a new point of view allows shedding a light on the relations between different physical fields and forces. An interdisciplinary study based on suggested concept leads to unveiling of hidden structural features of the elementary particles and atomic nuclei. The obtained physical models of the atoms exhibit the same energetic levels as the Quantum Mechanical models; however, the parameters and positions of the quantum orbits are strictly defined by the nuclear configuration. The derived models open a new possibility for analysis of sub-molecular and sub-atomic processes. The new concept allows finding logic behind quantum mechanical and relativistic phenomena. It logically leads also to a different hypothesis about the Universe, challenging the theory of Big Bang.

Keywords*: Zero point energy, vacuum, spacetime, unified field theories, physical structures of atoms, quantum orbits, embedded fine structure constant, molecular structures*

Note: For easy reference to the theoretical source, the numbering of equations and figures in square brackets matches the numbering in BSM thesis (first digit indicates the Chapter's number). The numbering of new equations and figures appears in a normal way.

1. The concept of the vacuum space as a key issue for building of unified field theory

One of the long standing problems in theoretical physics is how the gravitational field is related to the electrical and magnetic field. This is part of the problems related to development of successful unified field theory in order to understand better the real world. The building of such theory is dependable of the correctness of the adopted fundamental concepts and postulates in physics. One of them is the concept of the vacuum. Is the currently adopted concept about the vacuum space completely correct? Until the 17th century the Aristotel's view has been accepted, according to which the vacuum is a physically impossible. It has been overthrown after the invention of the barometer by Evangelista Torrichelli in 1644. The vacuum has been accepted as a pure empty space. This concept has been changed again in 19th century after the physicists discover the electromagnetic radiation.

In the last decades of 19 century the concept of the vacuum has been dominated by the aether theories. In the beginning of 20 century the aether theory has been ovethrown and replaced by the Einstein vision about the vacuum. In the article "Can Quantum-mechanical Description of Physical Reality Be Considered Complete?", A. Einstein, B. Podolsky and N. Rosen (1935) write: "Every element of the physical reality must have a counterpart in the physical theory." In one of its articles H. E. Puthoff, (1997) writes about the Einstein's view about his theory of General Relativity"

"With the rise of special relativity which did not require reference to such an underlying substrate, Einstein in 1905 effectively banished the ether in favour of the concept that empty space constitutes a true void. Ten years later, however, Einstein's own development of the general theory of relativity with its concept of curved space and distorted geometry forced him to reverse his stand and opt for a richly-endowed plenum under the new label spacetime metric".

In another article H. E. Puthoff (1997) provides a citation from A. Sakharov (the developer of russian hydrogen bomb) "Searching to derive Einstein's phenomenological equations for general relativity from a more fundamental set of assumptions, Sakharov came to the conclusion that

the entire panoply of general relativistic phenomena could be seen as induced effects brought about by changes in the quantum-fluctuation energy of the vacuum due to the presence of matter".

The “dark matter” is an extensively hot topic in cosmology today. Currently it is already accepted that the “dark matter” predominates the visible matter in the Universe. In recent years it has been found that in the centre of most of the galaxies there is a supermassive black hole in order of billion solar masses (keyword for search “supermassive black holes”). A surprising strong relation has been found between the mass of the supermassive black hole and the mass of the whole galaxy (L. Ferrarese, D. Merrit, 2000) It seams that this black hole know how much mass exists in the host galaxy or there is some kind of mass-energy balance. Additionally to this, one of the largest rotation curve data base of spiral galaxies clearly shows that the “dark matter” is rather a rule, than exception. (An analysis of 900 optical rotation curves: Dark matter in a corner?, by D. F. Roscoe, (1999)). Then it stands to reason raising a question: Isn’t the “dark” matter around us and even “within us” and if so isn’t the “hidden matter” more appropriate name? Then the concept of the vacuum should be inseparable from the concept of “dark” or “hidden” matter.

Large number of not solved problems and even mysteries in the range from particle physics to cosmology indicates that our current vision about the Nature and Universe may not present the real picture. This may lead to a serious gap between the fields of the theoretical physics from one side and applied sciences from the other. This is not an isolated opinion among the applied field scientists. In a recently published article “Physics in crisis” in Physics Today and FermiNews, Sidney Nagel (2002) points out the gap that now exists between the fields of fast advancing applied science and the particle physics. He writes; “So, in order to study geology, condensed matter physics, or biology, does one really need to know the standard model? Does it even help? Of course not.”

In the same perspective, we may take one example about the complex molecules, such as the organic and biomolecules. Despite the huge number of possible configurations of the atoms in such molecules they preserve their shape in proper environments. This is especially valid for the long chain biomolecules. If considering only the Quantum Mechanical considerations a protein molecule from 2,000 atoms, for example should possess an astronomical number of degrees of freedom. It is known, however, that this number is drastically reduced by some strong structural restrictions, such as bond lengths, relative bond angles and rotations. All this restrictions could not get satisfactory explanation by the Quantum Mechanical models of the atoms. This problem is known as a Levinthal’s paradox.

The above considerations and citations are presented only to show that the presently accepted concept about vacuum space could not be considered as a final truth. This may deform our knowledge about a large number of phenomena.

Inspired by the above considerations extensive search has been done about possible different concepts about vacuum that have not been studied so far. Apart of this a broad interdisciplinary study from different fields of physics and chemistry was done. It led to a conclusion that the Quantum Mechanical models may not show some structural features of the atoms. The search of alternative vacuum concept and the results of the interdisciplinary study led to development of original unified field theory called Basic Structures of Matter (BSM). In order to build such theory, however, the vacuum concept and some of the initially adopted postulates in modern physics had to be reconsidered. This led to derivation of quite different models of the atoms, possessing rich physical structures. The structural features are able to explain the observed length and angular restrictions of the chemical bonds. Such features are not apparent by the Quantum Mechanical models. In the same time, the physical models of the atoms exhibit the same energy levels and interaction properties as the Quantum Mechanical models. The valuable features of the derived models allows explanation of number of not solved problems in the fields of structural chemistry, biomolecules and the fast growing fields of nanotechnology.

The purpose of this article is to provide brief introduction into the concept and models of BSM theory. Without such introduction the potential of the these models for applications in different fields of applied science could not be understood.

2. The new point of view of the BSM theory

A new theoretical study, provided by BSM theory, indicates that the vacuum is not a void space, but possessing a underlying grid structure of super-dense particles. Extensive analysis of phenomena from different fields of physics allowed to formulate the search criteria for the possible physical model of this structure. Its properties must explain the basic physical effects in the complex "matter - energy - space - time - gravitation - fields". The search for the correct model took also into account number of recently published theoretical articles about the vacuum properties. They are related with some features, such as the Zero Point Energy, the quantum fluctuations and the polarizability of the vacuum. Number of theoretical works in this field are provided by T. H. Boyer, H. E. Puthoff, A. Rueda, M. Ibison, B. Haisch and others.

The defined criteria allowed to narrow the range of search, so one of the most promising model is suggested. According to this model, **the vacuum space possesses a underlying grid structure of sub-elementary particles arranged in nodes.** These particles called twisted prisms are formed of two types super dens intrinsic matter substances. Prisms of the same type are attracted in a pure void space by **Intrinsic Gravitational (IG) forces, F_{IG}, that are inverse proportional to a cube of the distance.**

$$F_{IG} = G_0 \frac{m_{o1} m_{o2}}{r^3} \qquad [(2.1)]$$

where: m_{o1} and m_{o2} are intrinsic masses (of this superdense particles), G_o is the Intrinsic Gravitational constant (there is an indication that it could be equal to the Newton's gravitational constant if the difference between the two type of intrinsic matter is taken into account), r - distance.

It is assumed that the IG force is related to the theoretically known physical parameter called Planck's frequency, ω_{PL}

$$\omega_{PL} = \sqrt{\frac{2\pi c^5}{G}} \qquad (1)$$

In the article "Gravity as a zero-point fluctuation force", H. E. Puthoff (1989) begins from the equation of the Planck's frequency and using one hypothesis of Sakharov successfully derives the Newton's law of gravitation. This result is used as a valuable initial point in BSM concept. Relying on the Planck's frequency as a real physical parameter is a step in a right direction in the process of building the BSM concept. The confidence about this is increased by the results obtained latter from the analysis of the derived models and their consistency with known physical parameters and experimental results.

Let focussing on the prisms and the single node of the introduced grid structure. The prisms are hexagonal sub-elementary particles with a length a few time larger than the diameter. They possess axial IG anisotropy with a twisting component, due to a lower level structure, so they are called twisted prisms. The dimensions ratio between the two types of prisms is 2:3. Every node is comprised of four prisms of same substance, normally at angle 109.5^o between them. The two types of nodes are alternatively arranged forming a grid similar as the atoms in a diamond. Governed only by the IG forces, the node geometry has some flexibility, while their mutual positions - some limited freedom. In some conditions part of the nodes could be displaced and folded, so they could pass through a normal grid structure. The IG field is a type of energy interaction between intrinsic matter at lower level of matter organization involved in an intrinsic energy balance. The gaps between the alternatively arranged nodes of different types are also results of an intrinsic energy balance. The estimated distance between neighbouring nodes of the grid is in order of (1 ~ 2)E-20 (m), while the matter density of the prisms is about 1E13 times higher than the density of the average atomic matter. This structure fills all the visible volume of the Universe. It is called a **Cosmic Lattice (CL)**, so the vacuum space in which we live and observe is referenced in BSM theory as a **CL space**.

The new concept about the vacuum broadens our vision about the space-time and matter-energy relations. Using the vacuum grid as a frame of reference, the BSM theory allows to separate the space from time parameters at low level of matter organization and to perform physical analysis in a real three dimensional space. In such approach the Quantum Mechanical rules and the relativistic phenomena are completely understandable and ex-

plainable by the human logic without need of the uncertainty principle.

The self-sustainable CL structure of the vacuum space is supported by super strong interactions between the highly dens prisms arranged in nodes. In the same time, the node distance is very weakly influenced by the atomic matter of massive astronomical objects. This effect is very weak because for the length scale range of CL node distance the Newtonian gravitation is negligible in comparison to the Intrinsic Gravitation. While the node distance is about 10E9 times smaller than the average internuclear distance of the atoms in a solid body, the matter density in the prisms is about 1E13 times higher than the average atomic matter. Therefore, the massive astronomical objects are able to influence the parameters of the surrounding CL space. This defines the local conditions of the light velocity, while the gradient of slightly affected node distance defines the General relativistic conditions.

Another specific feature of the CL space is the ability of the CL nodes to fold and pass through the grid structure of a normal CL space when a less massive object moves in a CL space of a more massive one. Such unique feature does not have counterpart in any concept of aether or ideal fluid.

The folding properties of the CL nodes is also closely related to the inertial properties of the atomic matter in CL space and plays a role in the equivalence between gravitational and inertial mass.

Analysing the dynamics and mutual interactions of the CL nodes (§2.9 of BSM), it is possible to understand some of the fundamental physical parameters, such as: unit charge, magnetic field, Planck constant, Zero Point Energy, photon wavetrain structure, light velocity, permeability and permittivity of vacuum.

Fig. 2.20 illustrates a geometry of a single node in position of geometrical equilibrium with two sets of axes, denoted as *abcd* and *xyz*.

The CL node has two sets of axes: one set of 4 axes along anyone of the prisms called *abcd* axes, and another set of 3 orthogonal axes called *xyz* axes. In geometrical equilibrium the angles between anyone of abcd axes is 109.5^{o}. The *abcd* axes define a tetrahedron. The *xyz* axes pass through the middle of every two opposite edges of the tetrahedron. In the same time, the orthogonal *xyz* axes of the neighbouring CL nodes are aligned.

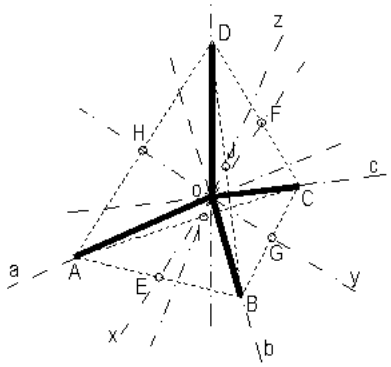

Fig. 2.20 CL node in geometrical equilibrium position The two sets of axes are: *abcd* and *xyz*

Such arrangement gives conditions for complex node oscillations under the inverse cubic law of intrinsic gravitation. The return forces (of inverse cubic law) acting on deviated from the central position CL node exhibits set of minimums. These minimums can be associated with energy wells. **Two symmetrical minimums appear along anyone of *xyz* axes and one minimum along the positive direction of anyone of *abcd* axes.** These set of minimums provide conditions for complex oscillations of the CL node. From a point of view of CL node dynamics they are responsible for the total energy well of the CL node (Zero Point Energy of vacuum). Fig. [2.24] illustrates the return forces along the two sets of axes and the associated with them energy wells.

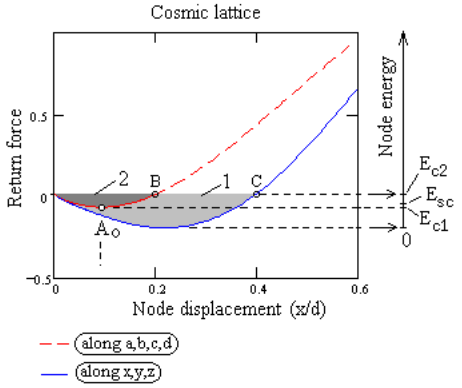

Fig. [2.24]

The right vertical axis indicates specific energy points. The energy level E_{C2} corresponds to the filled energy wells or the Zero Point Energy of the vacuum. The complex CL node oscillations are characterised by two types of cycles: a resonance cycle and a SPM cycle (the latter is described by a Spatial Precession Momentum vector). The trace of

the resonance cycle is approximately flat but open curve with four bumps, as shown in Fig. [2.26] The bumps are caused by the different stiffness between deviations along abcd and xyz axis (within finite angle). Therefore, the resonance cycle is characterized by a vector with for momentum maximums at two orthogonal axes. The points A and B from the resonance cycle are pretty close but not coinciding, so the segment AB points almost at 90 deg in respect to the drawing plane. The lack of coincidence between any initial (A) and final (B) point from one resonance cycle is a result of the asymmetrical spatial positions of the energy wells in respect to the central node point (node point for zero deviation).

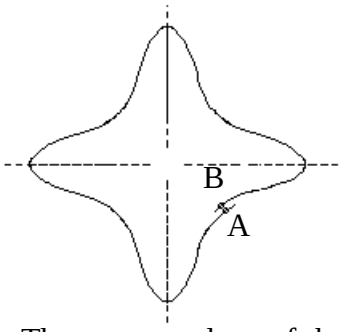

Fig. [2.26]

The average plane of the resonance trace is slightly rotated with every cycle, so after a large number of such cycles the node trace passes through the same (arbitrary selected) initial point A. This is a SPM cycle. The vector describing this cycle is called **SPM vector (Spatial Precession momentum)**. The number of the resonance cycle in one SPM cycle, estimated in BSM, is $N_{RQ} = 0.88431155 \times 10^9$.

The tip of SPM vector for one full cycle circumscribes a closed surface with central point symmetry and six bumps aligned along the axes xyz. Such type of surface is referenced in BSM as a **SPM quasisphere**. It is found that the resonance cycle is related to the velocity of the energy wave propagation (light velocity), while the SPM cycle is related to quantum features of the CL space. In such conditions, the SPM cycle is responsible for the constant light velocity, due to the quantum properties of the SPM quasispheres and their mutual interactions. The frequency of SPM cycle is equal to the known Compton frequency. In absence of any electrical charge, the SPM quasisphere possesses a central point of symmetry and it is called a **Magnetic Quasisphere (MQ)**. This is a normal state of the oscillating CL node that appears to be related to the magnetic permeability of the vacuum.

In presence of electrical charge, the SPM quasisphere obtains a deformation as an elongation along its diameter connecting two opposite bumps, so it is called an **Electrical Quasisphere (EQ)**. The shapes of MQ and EQ are shown in Fig. 1.

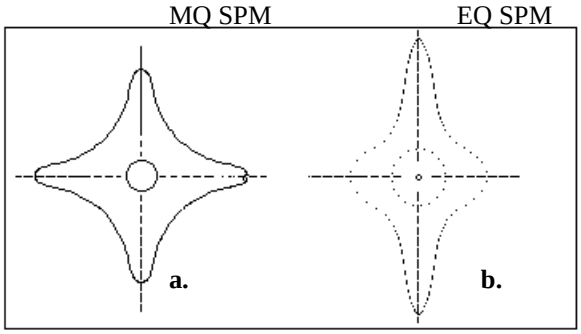

Fig. 1 MQ and EQ of SPM vector

By studying the dynamics of CL nodes it is found that the EQ type node possesses larger energy than MQ type. The electrical field is composed of spatially oriented and synchronized EQ CL nodes, so a domain of EQ type CL nodes possesses a larger energy than a domain of MQ type CL nodes.

From the other hand, **the magnetic field is a closed loop in CL space involving only MQ type of nodes whose SPM frequencies are synchronized.** Such arrangement, however, has some specific spatial and temporally features:

- The CL nodes of right handed prisms are commonly synchronized
- The CL nodes of the left-handed prisms are commonly synchronized
- The phase difference between the involved left and right handed nodes determines the direction of the magnetic field, for example, +90 deg phase difference for N-S direction and -90 deg phase difference for S-N direction.
- The involved MQ nodes may additionally have a helical arrangement along the closed loop

The above considerations are for permanent magnetic field. In case of alternative magnetic field, the commonly spatially dependable synchronizations of the left and right-handed stationary nodes vary with the time.

Physically the EQ type node is a stationary and defined by a local gravitational field of a massive object (in our case - the Earth). When studying the conditions of energy propagation as a wave, however, it is convenient to use **imaginary *running* CL nodes**. In such case the temporal variation of a common synchronization of the CL nodes are easily studied. The analysis in such approach led to unveiling the structure of the photon wavetrain as a complex but well defined spatial arrangement of EQ and MQ *running* nodes.

The photon wavetrain is a complex arrangement of *running EQs* with decreasing deformation gradient from the central axis of the wavetrain to its boundary radius, where *running MQs* are formed. Thus, it is found that the photon wavetrain has boundary conditions (a solution of one long standing problem).

The analysis of the CL node dynamics as EQ and MQ type and the unveiled photon wavetrain structure in a normal CL space (possessing a normal Zero Point Energy) are presented in Chapter 2 of BSM thesis. CL space with subnormal Zero Point Energy is related to superconductivity effects. The CL node dynamics and the charge particles behaviour in this state of the matter-space complex is analysed in Chapter 4 of BSM.

The applied new approach allows also unveiling the real physical structures of the atomic and subatomic particles. The Bohr atomic model appears to be only a mathematical model providing correct energy levels, but it is not identical to the physical one. When taking into account the vacuum structure and the structure of elementary particles, the physical models of the Hydrogen and all stable elements appear quite different.

From a BSM point of view, the interpretation of the scattering experiments does not provide correct real dimensions, because the structures of the vacuum and elementary particles are not taken into account. BSM analysis found that the stable particles, such as proton, neutron and electron (and positron) posses structures with well defined spatial geometry and denser internal lattices. They are comprised of complex but understandable three-dimensional helical structures whose elementary building blocks are the same as those involved in the vacuum grid - the two types of prisms. Analysing the interactions between the vacuum space and elementary particles, but from a new point of view, the BSM theory allowed a derivation of number of useful equations, such as a light velocity equation - expressed by the CL space parameters, a mass equation (the mass we are familiar with), an equation about the vacuum energy (zero point energy), and some relations between CL space parameters and the known physical constants. The BSM provides also an understandable physical explanation of what is an elementary electrical charge and why it is constant.

The motion analysis of the smallest charge particle - the electron from a new point of view (Chapter 3 and 4 of BSM) allows to unveil its physical structure and intrinsic properties. The electron is a system comprised of three helical structures as illustrated by Fig. 2. Two of its helical structures possess denser lattices located in the internal spaces of the helix envelopes (this lattice is not shown in Fig. 2).

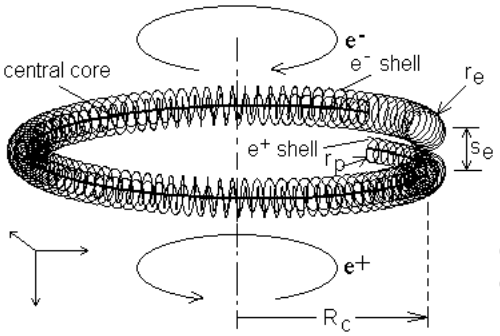

Fig. 2
Oscillating electron

The physical dimensions of this structures are: R_C - Compton radius of electron (known), r_e - a small electron radius, r_p a small positron radius, s_e - helix step.

External helical structure with internal denser lattice (from right handed prisms, for example) is referenced in BSM as external electron shell. It is responsible for the modulation of the CL space around the electron and creation of a negative charge. The internal helical structure with internal denser lattice (from a left-handed prisms, respectively) with a central core (from right handed prisms) is an internal positron. Regarded as a 3 body oscillating system the electron has two proper frequencies:

- a first proper frequency: between the external electron shell and the internal positron

- a second proper frequency: between the internal positive shell and the central negative core.

It is found that the first proper frequency of the electron is equal to the SPM frequency of the CL node. This is well known Compton frequency.

It is found that in conditions of screw-like motion of the electron with tangential velocity equal to the light velocity, the phase of the first proper frequency of the rotating electron matches the phase of the SPM vector. They both oscillate with a Compton frequency. In the same time, the internal core oscillation (with a proper frequency of three times the Compton frequency) provides a third harmonic feature for this motion. As a result the rotating and oscillating electron exhibit a maximum interaction with the CL space - a kind of quantum interaction. The electron axial velocity for this case is $V_{ax} = \alpha c$, corresponding to kinetic energy of 13.6 eV. In such type of motion the helical step, s_e, is given by the following expression:

$$s_e = \frac{2\pi R_c \alpha}{\sqrt{1-\alpha^2}} = \frac{\lambda_c \alpha}{\sqrt{1-\alpha^2}} = 1.7706\times10^{-14} \text{ (m)} \qquad [(3.9)]$$

$$s_e = g_e r_e = 2.002319 r_e \qquad [(3.12.a)]$$

where: R_c - is the Compton radius, α - is the fine structure constant, g_e - is the gyromagnetic factor, λ_c - is the Compton wavelength (CL space parameter).

From the analysis of the Fractional Quantum Hall experiments in Chapter 4 of BSM, it is found that: $r_p/r_e = 2/3$. Then all the of geometrical parameters of the electron are determined.

Electron confined motion with suboptimal velocities corresponding to $V_{ax} = \alpha c/n$ where n is a small integer is also possible but with decreasing strength of quantum interactions. They corresponds to kinetic energies of 13.6 eV. 3.41 eV, 1.51. eV, 0.85 and so on. The quantum conditions providing stabilizing effect for these velocities are discussed later.

The configuration of one of the internal lattices of the helical structures of the electron called a Rectangular Lattice (RL) is shown in Fig. [2.16]. Every RL node is comprised of six prisms of the same type. The axial section contains number of concentric layers. Starting from the cylindrical boundary defined by the helix envelope, the most external layer is connected to the helix by IG forces, while every internal layer is connected to the neighbouring external one. The thickness of every internal layer is half of the thickness of the neighbouring external layer. These are pure geometrical considerations for a stable internal lattice. The radially alined prisms of the neighbouring nodes are without gaps, while the gap between the tangentially aligned prisms varies when moving from external to the internal radius of the layer.

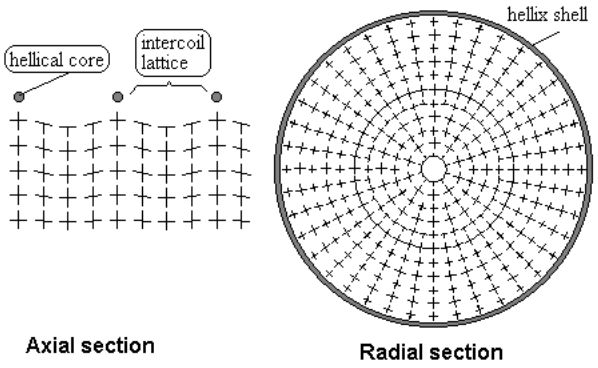

Fig. [2.16] Configuration of internal lattice of type RL (Rectangular Lattice) inside the cylindrical space enveloped by the first order helical structure

The electron structure, shown in Fig. 2 has two internal RL lattices. They are built of same type prisms like their envelope. The RL structure shown in Fig. 2 is the internal one and it possesses a central hole where the central core of the electron oscillates. The other RL lattice has a larger whole where the internal first order helical structure oscillates.

The stiffness of RL defined by the prism density is about 1000 times larger than the stiffness of CL structure of the vacuum. Consequently, the volume of RL structure is not penetrative even for folded CL nodes. Then it displaces the CL structure, or in other words, it feels a CL pressure. This is a Static CL pressure discussed later. For open helical structures like those in the electron (the both ends are not connected) the internal RL structure is stabilised by twisting. In such way, it becomes a twisted type of RL structure, denoted as RL(T). The twisted radial stripes of RL(T) modulate the CL nodes converting them to EQ type nodes arranged in a proper spatial configuration. It is evident that the modulated EQ nodes are arranged as lines extensions from the twisted radial stripe of RL(T). This is illustrated by Fig. [2.17]. These lines form the electrical field of the charge particle. It is evident that in a proximity range these lines might be slightly curved but in a far range they appear as emerging from a point. The line shape and

their connection to the twisted radial stripes of RL(T) is very important feature of the electron structure. It allows to explain magnetic type interactions of the electron moving in CL space.

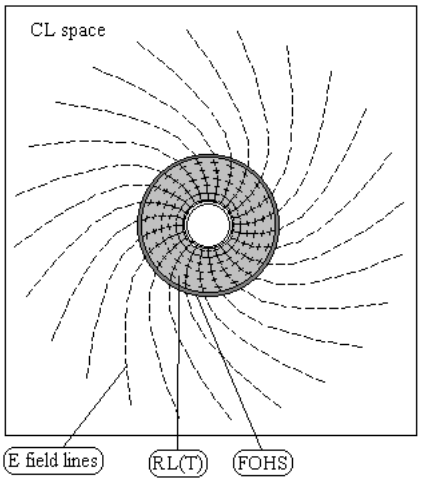

Fig. [2.17] Proximity E-field lines from RL(T) structure

It is apparent that one type of prisms (for instance the right handed) is associated with one sign of charge while other type with - another. Therefore we may address the two types of prisms as positive and negative, while keeping in mind that the physical charge appears only in CL space.

All elementary particles are built of helical structures that from their hand possess internal RL lattices. The RL and RL(T) parameters of the helical structures are determined in Chapter 6 of BSM, where physical meanings for number of experimentally obtained parameters from the particle physics are unveiled. This includes: the ratio between pion-muon mass, the tau particle (Regge resonance at 1.7778 MeV), the resonance at 1.44 MeV, the Fermi coupling constant G_F, the effective mixing parameter $\sin^2\theta_{eff}^{lept}$, the energy equivalence of the "masses" of the W+- and Z bosons.

By using the unveiled structure of the electron as a reference etalon, the basic parameters of the CL space are obtained and expressed by the known physical constants. The basic parameters are: the Static CL pressure - related to the Newtonian mass, the Dynamic CL pressure - related to the Zero point Energy of vacuum, the Partial CL pressure - related to the inertial properties of the atomic matter in CL space, the Compton frequency as a characteristic parameter of CL node and electron oscillating properties, the light velocity and the Compton wavelength. The obtained expression of Static CL pressure is:

$$P_S = \frac{m_e c^2}{V_e} = \frac{h\nu_c^4 g_e^2 (1-\alpha^2)}{\pi\alpha^2 c^3} \quad \left[\frac{N}{m^2}\right] \qquad [(3.53)]$$

The static CL pressure allows defining the Newtonian mass (the mass we are familiar with) for any particle in a stable phase of its existence.

$$m = \frac{P_S}{c^2} V_H \qquad [(3.48)]$$

where: V_e is the envelope volume of the electron and V_H - is the total volume of similar structures for a particle under consideration.

The energy from displaced CL nodes can be directly estimated by the Einstein's equation $E = mc^2$.

When the electron or any stable helical structure is in motion, it displays CL nodes. The displacement process for the stationary nodes involve the following phases: a node folding and displacement, a returning to the initial position and unfolding. There is not boundary between these two phases and the folding in partial. The displaced node preserves it energy momentum by converting the oscillation energy into rotational energy. In such conditions it may interact with the oscillating normal nodes. This is an inertial interaction that any moving helical structure exhibits in CL space.

A deeper study of this process leads to understanding the effects of Special relativity. It also leads to a conclusion (in Chapter 10 of BSM) that displaced nodes exist permanently around the atomic particles but only in motion in respect to the stationary CL space. The amount of the displaced nodes could be expressed by a CL space parameter Partial CL pressure. In Chapter 10 of BSM, where the inertial properties of the matter are discussed, it is found that the ratio between Partial and Static CL pressure is related to the fine structure constant by the relation:

$$P_P/P_S = \alpha^2/\sqrt{1-\alpha^2} \qquad [(10.18)]$$

The capability of the CL nodes to fold and penetrate in the normal CL space is one of the very specific feature related to the inertia of any particle in CL space. Therefore, it is involved in the definition of the inertial mass of the atoms and the matter

build of atoms. (On the other hand, the intrinsic matter possesses intrinsically small inertia in pure empty space, so it is possible to handle much larger energy. This is valid also for the CL structure).

The confined screw like motion of the oscillating electron in CL space is characterized by strong quantum interactions with the oscillating CL nodes. This effect is contributed by two conditions: a phase match between the involved cycles (discussed above) and conditions of integer number of Compton wavelengths for boundary conditions of the induced magnetic field from the rotating electron. These two conditions allow strong quantum effects to appear at particular velocities of screw-like motion of the electron, corresponding to the energy levels of 13.6 eV, 3.4 eV, 1.51 eV, 0.85 eV and so on.

The magnetic radius r_{mb} in a plane normal to V_{ax} is defined from the conditions that the rotating IG field of the internal lattice of the electron helical structure (that modulates the CL space) could not exceed the light velocity.

The magnetic radius for 13.6 eV is verified from the analysis of the quantum magnetic field (see §3.11 in Chapter 3 of BSM thesis): $\Phi_0 = h/q_o$ The accurate value of r_{mb} for 13.6 eV is almost equal to R_C, but slightly larger due to a finite thickness of the electron helical structure.

If relating the above energy levels with the number of full rotations of the electron one obtains:

13. 6 eV - 1 rotation per SPM cycle
3.4 eV - 1/2 rotations per SPM cycle
1.51 eV - 1/3 rotations per SPM cycle
0.85 eV = 1/4 rotations per SPM cycle
1 SPM cycle = Compton time

BSM uses a parameter called **subharmonic number**, *n*, in order to notify the quantum motion conditions of the electron. This number is related to the electron axial velocity by the expression $V_{ax} = \alpha c/n$. In the same time the subharmonic number matches the quantum number of the electron orbit in Bohr atomic model. A quantum motion with a first harmonic velocity corresponds to 13.6 eV, with a second subharmonic - 3.4 eV, with a third subharmonic - 1.51 eV and so on. The term subharmonic number is chosen because it annotates the spin rotation of the electron in its confined motion.

Analysing the efficiency of the quantum interactions between the confined moving electron and CL space at relativistic velocities the relativistic gamma factor is derived in §3.11.A. The analysis provides a physical explanation of the relativistic effect of mass increase. It is a result of the finite rate at which the CL node could be folded and displaced. A limiting factor of this rate is the resonance frequency of CL node, estimated in §2.11.3, Chapter 2 of BSM, as:

$$\nu_R = 1.092646\times10^{29} \text{ (Hz)} \qquad [(2.55)]$$

3. Quantum loops and possible orbits for electron with optimal confined velocity. Embedded signature of the fine structure constant.

3.1 Quantum motion of the electron in closed loop trajectories.

The motion of the electron is always a result of external forces. Such forces exists even without acceleration fields. The driving mechanism in such case is supported by the condition of accurately kept relation between the Static and Partial pressure of CL space, expressed by Eq. [(10.18)]. The partial pressure is contributed by the velocity and spin momentum of the folded nodes. They can exist only in motion. Therefore they are behind the driving mechanism that keeps the oscillating and orbital motion of the electrons in the atom. The orbital motion could be regarded as a motion in closed loop, whose trajectory follows equipotential surface of electrical field defined by one or more positive charges. All this conditions are ideal for a quantum motion of the electron in a closed loop.

Let considering a repetitive motion in a closed loop. Obviously, the length of such loop will depend of the conditions of phase matching between the SPM frequency of the CL node, from one side and the first and second proper frequencies of the electron, from the other. All of them can be expressed by the Compton frequency.

Let us find the path length at which the quantum loop condition for the electron moving with a first harmonic velocity (13.6 eV) is fulfilled. **Initially we will ignore the relativistic effect for simplicity.** It is reasonable to look for path length defined by some CL space parameter. One of this parameter is the Compton wavelength $\lambda_c = \lambda_{SPM}$

For one orbital cycle in a closed loop with length λ_c, the number of turns N_T is:

$$N_T = \lambda_c/s_e = 137.03234 \quad [(3.43.d)]$$

The value of N_T could be regarded as a condition of screw-like motion of the electron at which the initial phase in any one point of the closed loop is repeated. We see that it appears slightly different from the reciprocal value of the fine structure constant.

$$1/\alpha = 137.03598949$$

Therefore, the round number of turns is:

$$\overline{N_T} \approx 1/\alpha \quad [(3.43.e)]$$

The obtained number of turns as $1/\alpha$, however, is not a whole number. In the same time, the trace length of this loop is quite small, when comparing to the Bohr orbit length of $2\pi a_o$ (also with the proton dimensions determined in Chapter 6 as a result of the accepted concept of the vacuum space). Therefore, we may look for the phase conditions at larger loop length. The close value of N_T to $1/\alpha$ is not occasional. Then, one may substitute the N_T with $1/\alpha$ and multiply the result by λ_c that is associated with the circumference length of the electron coil. In such case we obtain:

$$N_T\lambda_c \approx \frac{1}{\alpha}\lambda_c = 3.249187\times10^{-10} \quad (m) \quad [(3.43.f)]$$

We see that the obtained value with dimension of length is equal to the Bohr orbit length:

$$2\pi a_o = 3.3249187\times10^{-10} \quad (m) \quad [(3.43.g)]$$

where: $a_o = 0.52917725\times10^{-10}$ (m) - is the radius of the Bohr atomic model of hydrogen.

The expression {(3.43.f)] is not something new. The important, fact, however, is the way of its derivation related with the suggested physical model of the electron. The obtained loop length appears equal to the orbit length of the Bohr atom. It is defined by Bohr atomic radius which is one of the very basic parameters used in the Quantum mechanics. From a point of view of BSM, however, the physical meaning of this parameter appears different.

According to BSM concept, the well known parameter a_0 used as a radius in the Bohr model, appears defined only by the quantum motion conditions of the electron moving in a closed loop with an optimal confined velocity corresponding to electron energy of 13.6 eV. Then the main characteristic parameter of the quantum loop is not its shape, but its length.

For a motion with optimal confined velocity the number of electron turns in the quantum orbit is equal to the orbital length $2\pi a_o$ divided by the helix step (s_e).

$$\frac{2\pi a_o}{s_e} = \frac{\lambda_c}{\alpha s_e} = 18778.362 \quad \text{turns} \quad [(3.43.h)]$$

The analysis of the confined motion of the electron in Chapter 3 and 4 of BSM indicates that its second proper frequency is three times higher than the first one (the first one is equal to the Compton frequency)

Let find at what number of complete orbital cycles (for orbit length of $2\pi a_o$) the phase repetition of the first and second proper frequencies of the electron is satisfied (in other words the smallest number of orbital cycles containing whole number of two frequency cycles). Eq. [(3.43.h)] shows that the number of first proper frequency cycle is close to 1/3. If assuming that it is exactly 1/3 (due to not very accurate determination of the participating parameters), then the condition for phase repetition of both frequency cycles will be met for three orbital cycles. The whole number of turns then should be $3\lambda_c/\alpha s_e$. Substituting s_e in this with expression given by Eq. [(3.9)] we must get a whole number of turns

$$\frac{3\sqrt{1-\alpha^2}}{\alpha^2} = integer \quad (2)$$

We have ignored so far the relativistic correction, but for accurate estimation it should be taken into account. The relativistic gamma factor for the electron velocity of $V = \alpha c$ is $\gamma = (1-\alpha^2)^{-1/2}$. Multiplying the above expression by the gamma factor we get.

$$3/\alpha^2 = integer \quad (3)$$

Eqs. (2) and (3) provide a possibility for verification of the phase repetition condition if the accuracy of the experimentally estimated fine structure constant exceeds some threshold level. The procedure is simple: calculation the expression by the recommended value of α, rounding the result to the closer integer and recalculating the corresponding value for α. The whole number of turns condition could be correct only if the recalculated value is in the range of the accuracy of the experi-

mentally determined α. The recommended value of α according CODATA 98 is

$$\alpha = 7.2973525(27)\times 10^{-3} \quad \text{(CODATA 98)} \qquad (4)$$

where the digits in bracket is the uncertainty error.

The calculated values of α from Eq. (2) and (3) exceed quite a lot the uncertainty value of experimentally determined α given by Eq. (4). Consequently, the condition of phase repetitions of the two proper frequencies is not fulfilled for three orbital cycles with total trace length of $3\times 2\pi a_o$. Therefore, we may search for the smallest number of orbital cycles in which the phase repetition conditions are satisfied. It stands to reason that the approximate value of the orbital cycles could be about 137 ($1/\alpha$). Then if not considering relativistic correction, the number of electron turns is

$$\frac{\sqrt{1-\alpha^2}}{\alpha^3}$$

When applying relativistic correction (multiplying by relativistic gamma factor) the number of electron turns is $1/\alpha^3$. The phase repetition conditions will be satisfied if this number is integer.

$$1/\alpha^3 = integer \qquad [(3.43.i)]$$

Substituting α with its value from CODATA 98 (Eq. (4)) we get

$$1/\alpha^3 = 2573380.57$$

For plus and minus deviation in a range of uncertainty error (value in brackets in Eq. 4)) we get respectively 2573380.55 and 2573380.6.

Consequently, we may accept that the full number of turn is 2573380.

It is evident that theoretical expression [(3.43.i)] can be used only if the experimental accuracy exceeds some threshold. Then the more accurate theoretical value is:

$$\alpha = (2573380)^{-1/3} = 7.2973531\times 10^{-3} \qquad (5)$$

The small difference of the theoretically obtained value of α from the experimental one is likely caused by the method of its determination by experiments. One of the most useful expression for experimental estimation is based on the measurement of the Josephson constant, K_J. Its connection to α is given by the expression, where all other physical parameters are known with high accuracy.

$$K_J = \frac{2}{c}\sqrt{\frac{2\alpha}{\mu_o m_e \lambda_c}} \qquad (6)$$

where: μ_o - is the permeability of vacuum, m_e - is the electron mass, c - is a light velocity, λ_c - is the Compton wavelength.

The accuracy of α according to this method depends of the accuracy of the Josephson constant measurement. The recommended value for this constant according to CODATA 98 is $K_J = 483597.898(19)\times 10^9$ (hz/V)

If substituting in Eq. (6) the recommended by CODATA 98 value of alpha with the calculated one by Eq. (5), the value of the Josephson coefficient is still in the uncertainty range (shown in brackets).

From the following later analysis we will see that it is more appropriate to use the number of full cycles of the first and proper frequencies. They are completely defined by the quantum velocity of the electron and the orbit trace length. In such way we arrive to the conclusion:

(A) The number of cycles of the first and second proper frequency of the electron in the orbital trace is defined only by the fine structure constant.

The conclusion (A) is reasonable from a physical point of view when having in mind the dynamical interactions between the oscillating electron and the oscillating CL nodes from one side and the embedded fine structure constant in the electron structure from the other.

The integer value 2573380 is proposed also by Michael Wales, based on quite different method for analysis of the electron behaviour (See Michael Wales book “Quantum theory; Alternative perspectives”)

The introduced subharmonic number (n) corresponds to the principal quantum number of Bohr model. The magnetic radius of electron motion with different number *n* is analysed in §3.1 (Chapter 3 of BSM). Its value for $n = 1$ matches to the estimated magnetic radius corresponding to the magnetic moment of the electron. For larger numbers, however, the magnetic radius shows and increase. The physical explanation by BSM is that at decreased electron rotation its IG field of the twisted internal RL structure is able to modulate the surrounding CL space up to a radius until the rotating modulation of the circumference reaches the speed of light. At this moment the circumference length of the modulation boundary is equal to a whole

number of Compton wavelengths. These conditions in fact define the stable velocity at any one value of subharmonic number *n.*

Table 1 shows the quantum motion parameters of the electron in a quantum loop for velocities corresponding to different subharmonic numbers.

Table 1

No	E (eV)	V_{ax}	V_t	r_{mb}	l_{ql}	L_q (A)
1	13.6	αc	c	$\sim R_c$	$2\pi a_0$	1.3626
2	3.4	$\alpha c/2$	$c/2$	$2R_c$	$2\pi a_0/2$	0.6813
3	1.51	$\alpha c/3$	$c/3$	$3R_c$	$2\pi a_0/3$	0.4542
4	0.85	$\alpha c/4$	$c/4$	$4R_c$	$2\pi a_0/4$	0.3406
5	0.544	$\alpha c/5$	$c/5$	$5R_c$	$2\pi a_0/5$	0.2725

where: E - is the electron energy, V_{ax} - is the axial velocity, V_t - is the tangential velocity of the rotating electron structure, r_{mb} - is the value of the boundary electron magnetic radius in a plane normal to V_{ax} vector, c - is a light velocity, R_c - is the Compton radius, a_o - is the Bohr radius, l_{ql} - is the trace length for a motion in closed loop (single quantum loop), L_q - is the length size of the quantum loop as Hippoped curve with parameter $a = \sqrt{3}$

The introduced parameter **subharmonic number** shows the rotational rate of the whole electron structure. The rotational rate decreases with the consecutive increase of this number, but the number of the first and second proper frequency cycles is not changed. This is very important feature formulated by the conclusion (B).

(B) The number of first and second proper frequency cycles of the electron in closed loop with any subharmonic number is a constant.

From the provided analysis we find that the electron makes 18778.362 rotations for one quantum loop. One quantum orbit may contain one ore more quantum loops. From Table 1 we see that for a confined moving electron the circumference length of the boundary of the electron's magnetic radius in a plane normal to V_{ax} is equal to a whole number of λ_c

While the Compton frequency, ν_c, expresses the frequency of the SPM vector and the first proper frequency of the oscillating electron, the Compton wavelength, λ_c, is a characteristic parameter of CL space related with the light velocity by the simple relation $\lambda_c = c/\nu_c$. The frequency of SPM vector from its side is directly related to the known physical parameter **permeability of vacuum.**

3.2. Quantum orbits. Emission and absorption of photon.

It is apparent from the provided analysis that a stable quantum loop is defined by the repeatable motion of oscillating electron. The shape of such loop is defined by external conditions. Such conditions may exist in the following two options:

- a quantum loop obtained between particle with equal but opposite charges and same mass, as in the case of positronium (see Chapter 3 of BSM)

- a quantum loop obtained between opposite charges but different masses (a hydrogen atom as a most simple case and other atoms and ions as more complex cases).

In both options the quantum loops are repeatable and we may call them **quantum orbits**. The quantum orbit may contain one or few serially connected quantum loops. It is obvious that the shape of the quantum orbit is defined by the proximity field configuration of the proton (or protons). The vacuum space concept of BSM allows unveiling not only the electron structure but also the physical shape of the proton with its proximity electrical field. The shape of any possible quantum orbit is strictly defined by these proton's parameters.

The conditions defining the quantum orbit allow unveiling the parameters of the possible quantum orbits in atoms and molecules. The most simplest examples are the possible quantum orbits of hydrogen atom. In Chapter 7 of BSM a model of Balmer series is suggested. Its analysis confirms the concept of confined motion of the electron. The trace length of the quantum orbit of Balmer series matches the quantum loop No 2 from Table 1. The same quantum loop exists also in Deuteron. The BSM model of Hydrogen is different from the Bohr model, but all quantum numbers and their energy levels are identifiable. The principle quantum numbers are obtainable by considering a whole number of Compton wavelengths but in specific environments defined by the proximity distributed E-field of the proton and the proton's Intrinsic Gravitational field.

It appears that the limiting orbit has a length of $2\pi a_0$ and all other quantum orbits are inferior.

This is valid not only for Balmer series in Hydrogen but also for all possible quantum orbits in different atoms, if they are able to provide line spectra. Therefore, the obtained physical model of Hydrogen provides **a solution of the boundary conditions problem of the electron orbits.** Similar solution exists for all atoms.

The analysis of interactions between the oscillating electron in confined motion and oscillating CL nodes allows unveiling the process of the photon generation. According to the BSM concept, the emission of photon contributing to a particular spectral line is a result of **pumping of CL nodes** from the orbiting and simultaneously rotating and oscillating electron. In this process usually more than one orbital cycles are involved. **The emission of a photon occurs from the surrounding CL space in the moment when the electron drops from higher to lower energy orbit.**

This explains why the Quantum Mechanical model needs the Heizenberg's uncertainty principle, while the BSM model does not need such one. In Quantum Mechanical models the CL substance is missing and the process of the photon generation has to be directly connected to the orbiting electron. In such case, it seems that the electron position could not be located, so a concept of "electron cloud" is used. In BSM modes of the atoms every electron is moving in orbit with well defined spatial parameters, so its motion could be theoretically analysed in any point of this orbit.

Fig. [7.19] illustrates the close match between the energy levels calculated by BSM model of Balmer series in Hydrogen and those provided by the Quantum mechanics.

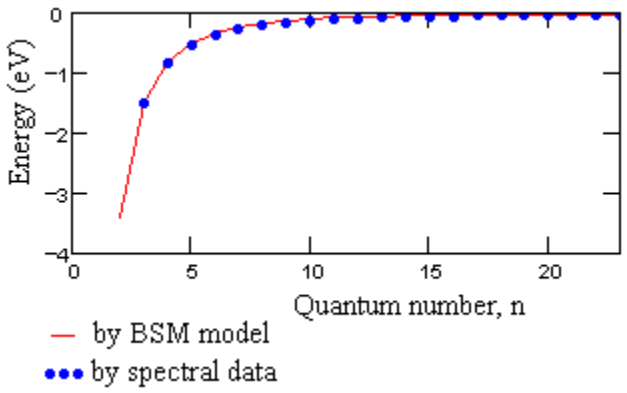

Fig. [7.19] Comparison between calculated and experimental energy levels for Balmer series

The electron with unveiled structural parameters is used also as a probe for estimation of the CL space parameters and formulation of mass equation valid for Newtonian gravitation and mass (the gravitation and mass we are familiar with). The Newtonian gravitation (known also as universal gravitational law) appears as a field of the Intrinsic Gravitation in CL space, where IG forces are propagated through the CL structure.

3.3 Lifetime of the orbital motion of the electron

In section 3.1 it was found that the condition for phase repetition of the two proper frequencies of the electron with velocity $V = \alpha c$ (13.6 eV) are accurately met for 2573380 electron turns (about 137 orbital cycles) and approximately met for three orbital cycles. The full travel of the rotating electron in both cases can be expressed by the product of the number of turns and helical step. Taking into account the relativistic gamma correction the full travel is $(1/\alpha^3)\times s_e$. In the same time the quantum velocity of the electron is known. Then dividing the full travel by the velocity one obtains the orbital lifetime.

$$\tau_{sp} = \frac{3\lambda_c}{\alpha^3 c\sqrt{1-\alpha^2}} = 6.248\times10^{-14} \text{ (s)} \qquad (7)$$

For a second harmonic quantum loops the number of electron turns is twice smaller, so its velocity and travel length are also twice smaller and the lifetime appears the same. **Consequently the obtained equation (7) appears valid for a quantum orbit with any subharmonic number, *n*, and comprised of single quantum loop** (as shown in Table 2). It is quite reasonable to consider this to be the lifetime for spontaneous emission. For quantum orbit comprised of *m* number of quantum loops the lifetime will be *m* times larger. Such conditions appear for the higher order series of Hydrogen in respect to the Balmer series.

In case of simulated emission, the lifetime of the orbiting electron could be shortened. It is interesting to find what could be the shortest lifetime in which a photon generation is still possible. From Eq. [(3.43.h)] we see that this could be the lifetime corresponding to three orbital cycles. Proceeding in a similar way as for the spontaneous emission we arrive to the result

$$\tau_{min} = \frac{3\lambda_c}{\alpha^2 c\sqrt{1-\alpha^2}} = 4.5596\times10^{-16} \text{ (s)} \qquad (8)$$

Note: The simplified equations (7) and (8) do not take into account the relativistic considerations.

Summary:

- The orbital lifetime for spontaneous emission is the time for which the first electron frequency makes 2573380 cycles
- The shorter lifetime for simulated emission is the time for which the first electron frequency make 18778.3 cycles (the secondary electron frequency makes 56335 cycles)

4. External shape and geometry of the proton and neutron

It is known from the particle physics experiments that the electron (positron) is an end product in the most frequent reactions of the type: pion - muon - electron (positron) or charged kaon - pion - muon - electron (positron). This feature allows using the unveiled structural and interaction parameters of the electron in order to solve the inverse task: to restore and find the physical structures of muon, pion, kaon and finally the structure of the stable particles proton and neutron. For this purpose, the derived mass equation Eq. [(3.48)] and its modification are used in the analysis provided in Chapter 6 of BSM. When applied for the proton, the parameter V_H takes into account the total volume of all helical structures defined by the volume of their internal Rectangular Lattice. The unknown parameters of mass budget are obtained by using accurately measured experimental data from particle physics but applied according to their correspondence to the unveiled physical models, according to BSM. One still missing parameter for solution of the necessary set of equations is the length of the proton central core (L_{PC}). It, however, participates in the proton envelope that is found out to be involved in a permanent interaction process with a Zero Point Waves of CL space. It is found that these waves, permanently persistent in CL space, are directly related to the background temperature of CL space. A theoretical expression of this temperature is derived in Chapter 5 of BSM by using the concept of Zero Point Waves (ZPW) bouncing on the envelope surface of the proton. In conditions of dynamical equilibrium, the energy of the bouncing ZPW is equal to the energy radiated from the atoms and molecules, dispersed in the interstellar space. The signature of this process according to BSM concept is the measured Cosmic Microwave Background (CMB) corresponding to temperature of 2.72 K. In the derivation of the theoretical equation of this temperature the following physical laws and parameters are involved: the ideal gas law, the Avogadro number, the proton geometrical parameters, the relation between the magnetic moments of electron and neutron (neutron is used more accurately instead of proton in order to reflect the neutrality of the involved atoms and molecules contributing to the CMB).

$$T = \frac{N_A^2}{S_W}\frac{h\nu_c(R_c+r_p)^3 L_{pc}^2}{2cR_c r_e R_{ig}}\left(\frac{\mu_e}{\mu_n}\right) = 2.6758 \text{ K} \qquad [(5.8)]$$

where: $S_W = 1\ m^2$ participates as a reference surface in SI system, μ_e and μ_n - are the magnetic moments of electron and neutron, respectively.

The approximate determination of the L_{PC} from Eq. [(5.8)] allows to solve a set of mass budget equations in Chapter 6 of BSM. In these equations, some additional data are used from the particle physics, such as: the mass of eta particle, the antiproton/proton ratio of stopping power, and the energy-mass equivalence of W bosons and tau particle. The calculations allow accurate determination of the proton (neutron) geometrical parameters and its internal structure. The proton is a twisted loop hardware structure with a curled shaped external helical structure of positive prisms. Inside this envelope there are two pions (positive and negative) also with shapes of curled twisted loops but with larger secondary helical step. One central kaon structure has a similar shape as the envelope of the twisted proton. When the proton is broken in one place (means the hardware loop is cut) its positive external helical structure envelope is usually firstly destroyed (releasing a huge IG energy from the dens internal RL structure). The internal so far pions and kaons are released and they are also broken in one place but in this configuration they are not stable. More often, the kaon decay into pions, and the pions decay into muon, whose shape is like a multiturn electron (or positron) structure. Then the decay of muon is accompanied by destruction of its internal Rectangular Lattice

(also twisted) that is much denser than the Cosmic Lattice. During this process an enormous energy is released. This energy gives the infinities in the Feynman diagrams. Some signatures of released energies from RL destruction of helical structures, for example, are the following: the experimentally estimated energies corresponding to the "mass" of W^- and W^+ bosons (from the kaon structures, according to BSM); the experimentally measured energies corresponding to the "mass" of the tau particle and the Regge resonance at 1.44 GeV (both from the helical structures of the normal electron, according to BSM). All high order helical structures are built of same lower order helical structures similar as the single turn structure of electron (with internal lattice) but they are multiturn, instead. The parameters r_e and r_p of all type helical structures, however, are the same (slightly different only for the internal pions and kaon because of their different degree of twisting).

The briefly described process of proton destruction occurs in experiments provided by particle colliders. One important feature that has been initially understood in BSM analysis is the strong and narrow Regge resonances (term in particle physics experiments) providing a logical indication that a **hardware loop is broken in one place and internal hardware loops also broken in one place are released.**

The proton core length (L_{PC}) participating in Eq. [(5.8)] is cross-validated by the Balmer series model (Chapter 7 of BSM) and by vibrational models of some simple molecules (Chapter 9 of BSM).

The proton is a loop of finite thickness twisted in a shape of figure 8, while the neutron is a same structure but with a shape of double folded loop. More accurately the plane projection of the proton envelope is quite close to a Hippoped curve with parameter $a = \sqrt{3}$. The twisting (and folding) direction is strongly defined by the underlined structures of pions and kaon inside the proton (neutron) envelope. Consequently all protons (and neutrons) involved in atomic nuclei have one and a same handedness (direction of twisting) but different degree of twisting). The shapes of the proton and neutron are shown in Fig. 3.

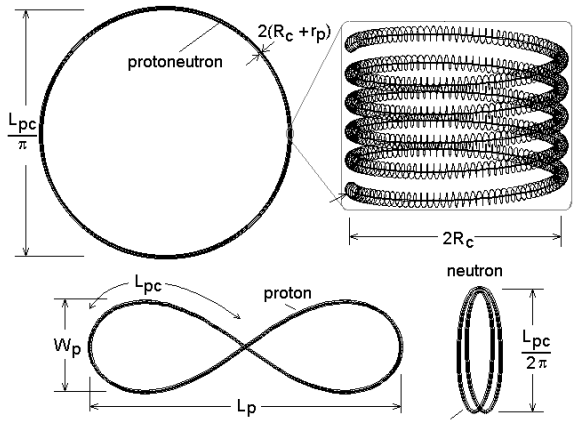

Fig. 3. Geometrical parameters of the proton and neutron. The magnified view shows only the external helical shell without the internal structures of pions and kaon (extraction from Atlas of ANS)

The estimated geometrical parameters of the proton (neutron) and electron are given in Table 2.

Physical dimensions of stable elementary particles Table 2

Parameter	Value (m)	Description	Reference BSM Chapter No.
L_{PC}	1.6277E-10	*p* and n core length	5, 6
L_P	0.667E-10	*p* length	6, 7, 8, 9
W_P	0.19253E-10	*p* width	6, 7, 8, 9
r_e	8.8428E-15	small radius of e^-	3, 4, 6
r_p	5.8952E-15	small radius of e^+	3, 4, 6
s_e	1.7706E-14	e^- (e^+) helix step	3
R_c	3.86159E-13	e^- Compton radius	Known
$2(R_c + r_p)$	7.8411E-13	*p* and *n* thickness	6, 7, 8, 9

Notations:
p - proton, *n* - neutron, e^- - electron, e^+ - positron

The calculated physical dimensions of proton and neutron appear quite different from those obtained by the scattering experiment. However, important factors such as the vacuum grid and the particle structures are both not taken into account in the interpretation of these experiments so far. The proton and neutron both have exactly the same internal structure, so they are distinguishable only by their overall shape (and a slight difference in their internal structural twisting that provides a slight mass difference). Then a question may arise: why the proton possesses a charge while, the neutron - not. The answer is: The electrical charge is a

result of the modulation of the surrounding CL nodes by the RL(T) lattice of the helical structures (external shells). In case of neutron, all helical structures get overall symmetry in respect to its axis. For such shape, the modulation of CL space in the far field is compensated and the electrical field is a zero. In case of proton, the overall torus is twisted and the axial symmetry of RL(T) is destroyed. Therefore, it is able to modulate the CL node in the near and far field.

Fig 4 shows the spatial geometry of the Deuteron, where: *p* - is the proton and *n* - is the neutron. The neutron is centred over the proton saddle and kept by the Intrinsic Gravitation (IG) field and the proximity electrical fields of the neutron and proton. In such conditions the neutron is kept stable (it is not able to unfold and convert to proton).

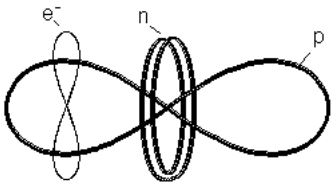

Fig. 4. Deuteron with electron in Balmer series according to BSM physical model

Fig. 5 illustrates the protons and neutrons arrangement in the nucleus of He. In such close distance, the internal lattices of the proton's helical structures are kept by IG forces that are inverse proportional to the cube of the distance. The nucleus of helium is the most compact atomic structure. Therefore, its influence on the CL space parameters in comparison to other atomic structures is the strongest one. As a result, the helium nucleus possesses the largest binding energy between the involved protons and neutrons. .

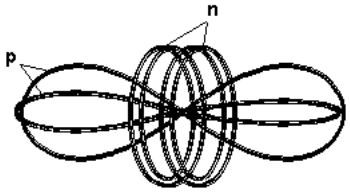

Fig. 5. Helium nucleus according to BSM physical model

When taking into account the two features of the proton: a finite geometrical size and the distributed proximity electrical field it is evident that the Coulomb law is valid down to some limit, defined by the finite size of the proton structure. This is verified by the model of Balmer series in Hydrogen presented in Chapter 7. The idealized shape of Balmer series orbit is shown in Fig. [7.7].

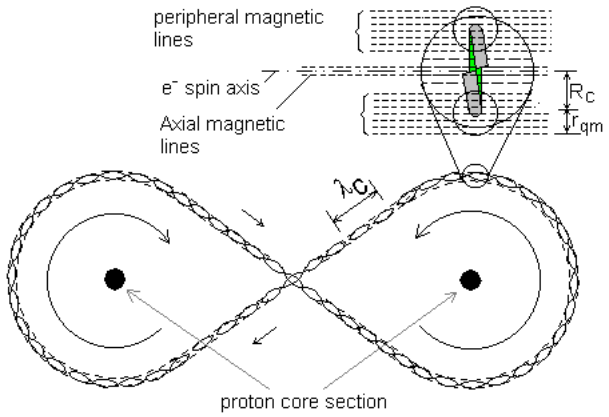

Fig. [7.7]. Idealized shape of Balmer series orbit. R_C - is the Compton radius, r_{qm} - is a magnetic radius of electron at sub optimal quantum velocity. The Compton wavelength λ_c shown as standing waves is is not in scale

5. Atlas of Atomic Nuclear Structures

5.1. Physical atomic models according to BSM concept.

One of the most useful results of BSM theory with practical importance is the Atlas of Atomic Nuclear Structures (ANS). The analysis leading to unveiling the spatial arrangement of the protons and neutrons in atomic nuclei is provided in Chapter 8 of BSM. It is found that the protons and neutrons follow a strict spatial order. This order is connected to well defined building nuclear tendency related to the Z number of the elements. The signature of this tendency matches quite well the row-column pattern of the Periodic table, the Hund's rules and the Pauli exclusion principle. The Atlas of ANS provides nuclear configurations of the elements from Hydrogen to Lawrencium (Z = 103). For drawing simplification of the nuclear structures, the protons and neutrons are presented by simplified patterns reminding their shape. The left part of Fig. 6 shows the patterns used for the proton, deuteron, tritii and helium, while the right part shows the most common shapes and possible dimension of the quantum orbits. The dimensions of the quantum orbits and the proton and neutron are given in one and a same scale.

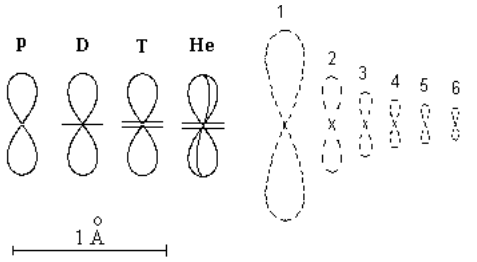

Fig. 6

Patterns for simple elements and quantum orbits

For any atomic nucleus, a polar axis is identifiable. It is defined by the long symmetrical axis of one or more He nuclei that are always in the middle of atomic nucleus. The atomic nuclei posses also twisting features due to the proton twisting, but it is not shown in the drawings. In the Atlas of ANS, the pattern of proton is symbolized by arrow in order to simplify the drawings. Additional symbolic notations are used for the the different types of bonds and pairing in which IG and EM fields are involved.

5.2. Three-dimensional structure of atomic nuclei and limited angular freedom of the valence protons.

The Atlas of Atomic Nuclear Structures provides the nuclear configurations of the stable isotopes. One or more He nuclei are in the nuclear centre, aligned with the polar axis of symmetry. The peripheral building blocks of the lighter elements are usually deuterons, while the element tritii appears more frequently in the nuclei of heavier elements. The positions of the protons are defined by the consecutive number of proton's shell and by the type of the bonds between the protons. Fig [8.2] illustrates the backbone structure of nucleus allowing the most dens pack of the protons and neutrons, having in mind the opposite forces keeping their positions: the attractive IG forces and the repulsive electrical forces between the proximity fields of the protons and the neutrons. The chain structure appears for the atoms with Z > 18 (after Argon).

The structural restrictions of the positions of the atoms in the molecules comes from two factors:

- stable structural arrangements of the bonded protons of the nucleus
- angular restrictions of the valence protons

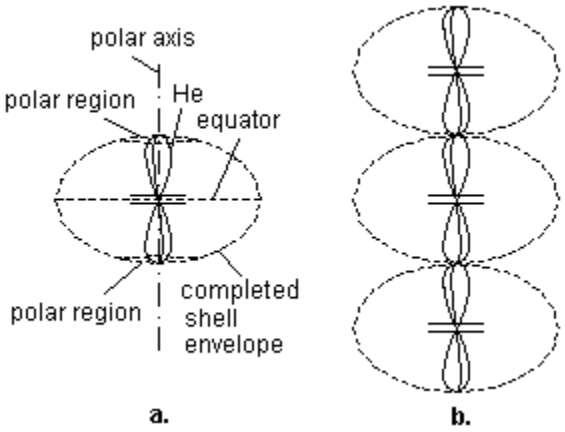

Fig. [8.2]

a. - polar structure; b. - polar-chain structure

The unveiled type of bonds between protons and neutrons in the atomic nucleus are given by Table 3. The gravitational bonds are held by the IG field of the intrinsic matter (more explicitly the IG field of the internal lattices of the helical structures from which the proton and neutron are built). The IG field controls also the proximity E-field of the proton (and proximity locked E-field of neutron) and its unity charge appearance. For this reason, all GB types of bonds are very stable.

Bonds in the atomic nuclear structure **Table 3**

Bond notation	Description
GB	Gravitational bond by IG forces
GBpa	polar attached GB
GBpc	polar clamped GB
GBclp	(proton) club proximity GB
GBnp	neutron to proton GB
EB	electronic bond (weak bond)

The four different types of the gravitational bonds and one type of electronic bond are illustrated in Fig. [8.4], where the positions of some quantum orbits are also shown. The GBpa bonds for valence protons have an angular restricted freedom of motion in a plane close to the polar section. Protons (deuterons) held by GBpa and GBclp bonds do not have any freedom of motion. The EB type of bonds are valid only for the valence protons but they are provided by electron orbit pairing, corresponding to the Hund rules. There are few types of such pairings. The two of them are more important:

a first type - two orbits in separated parallel orbital planes; a second type - a single orbit with two electrons with different QM spins, according to a Pauli exclusion principle (they are orbiting in opposite directions). The second type of Hund rule appears valid for EB bonds.

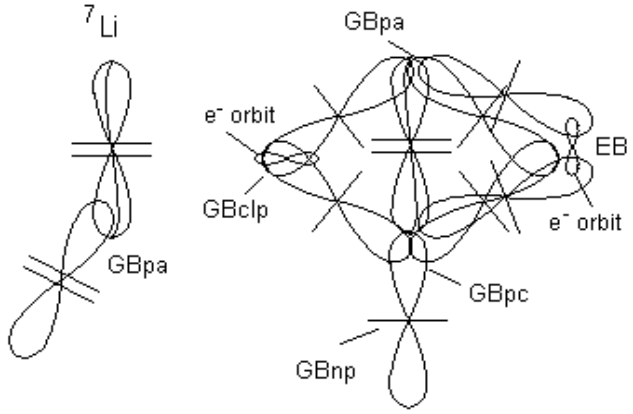

Fig. [8.4] The left-side structure is ^{7}Li nucleus,. The right-side structure is only a portion of nucleus showing the different type of bonds, according to Table 3. The planes of the shown quantum orbits are normal to the drawing plane.

The GB type bonds could not be broken in any type of chemical reaction, but only in nuclear reactions where quite large energies are involved. The EB type of bond however is weak. Bonds of such type begin from the raw 13 of the Periodic table while in raw 18 (noble gazes) they are converted to GBclp bonds. The EB bonds normally exclude the external shell protons from chemical valence, so they play a role for the principal valence of the elements from group 13 to 17. This is valid for rows 1, 2, 3 of the Periodical table. In some conditions, however, the EB bonds could be broken, so the element may exhibit multiple oxidation numbers.

For some chemical compounds between elements with large number of valence protons, not all of them can be connected by electronic bonds. This is a result of the finite nuclear size of the atoms and the angular restriction of the valence protons.

It is evident from the nuclear structure that **the positions of the electron orbits are strictly determined by the positions of the protons with their proximity electrical fields and the conditions of quantum orbits provided by Table 1.** Therefore, the electron orbits are not shown in the Atlas of ANS but their positions are easily identifiable. Having in mind the above consideration the well defined orbital positions are characterized by the same first ionization potential embedded in the Quantum Mechanical models and obtained experimentally.

6. Electronic bonds between atoms in molecules

It is evident that the BSM model of the atom allows identification of the orbital planes and chemical bond orientation of the atoms when connected in molecules. Additionally the Quantum Mechanical spin of the orbiting electron in respect to the proton twisting is also identifiable. The proton envelope is twisted torus, so it possesses a well-defined handedness along any one of its axes of symmetry. Then, the electron in the quantum orbit shown in Fig. 4 has an option to move in two different direction in respect to the proton direction of twisting. This will correspond to two slightly different energy levels for one and a same quantum number. **Its signature is a fine structure splitting of the spectral line.**

The intrinsic conditions of the quantum orbits defined by the two proper frequencies of the electron and the CL space properties are valid also for the bonding electrons in molecules. Let considering the most simple case of H_2 molecule identified as an ortho-I state. Its shape is illustrated in Fig. [(19.2)].

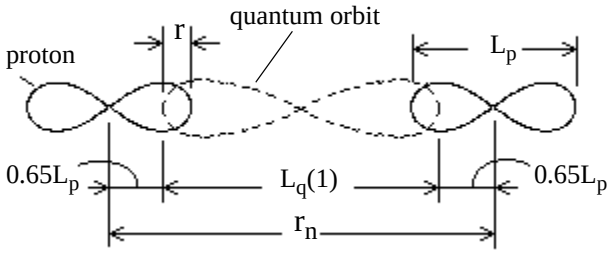

Fig. [9.12] Structure of H2 - ortho-I state molecule
L_p - is a proton length
$L_q(1)$ is a long side of a first harmonic quantum orbit
r_n - is the distance between the Hydrogen atoms
r - distance between the electron and the proton's core in the circular section (for the most external orbit
Note: The quantum orbit quasiplane is perpendicular to the quasiplane of the protons. However, they both are shown in one plane for simplification of the drawing

In this figure, the three-dimensional shape of the proton is replaced, for simplicity, by a 2-dimen-

sional Hippoped curve with parameter $a = \sqrt{3}$. The molecular vibration in such simple system is of linear type. The long axes of the protons and quantum orbit are aligned with the molecular vibrational axis. The both electrons move in a common quantum loop (orbit) but in opposite directions (opposite QM spins). The quantum orbit crosses the Hippoped curves of the protons in the locus points. We may assume that every orbiting electron is able to neutralize one charge, by interconnecting its E-filed lines to the proton E-field. Let considering the moment, when both electron are in the locus points of the Hippoped curves, representing the protons. Their velocity vectors in this case are perpendicular to the direction of the molecular vibration and do not contribute to the momentum energy of the system. Then, their moment interaction can be estimated by considering only two unit charges at distance r_n. Now, let assume that the left proton and the right electron are both missing. The system energy in this case is $q/4\pi\varepsilon_o r_n$ [eV]. The same considerations and results are valid also for the other symmetrical case. Adding the energies from the two symmetrical cases we get the full system energy.

$$E = \frac{2q}{4\pi\varepsilon_0[L_q(1) + 0.6455L_p)]} = 16.06 \text{ eV} \qquad [(9.40)]$$

where: the factor 0.6455 defines the distance of the locus from the central symmetrical point of the Hippoped curve with factor $a = \sqrt{3}$.

7. Vibrational motion of atoms connected in molecule by electronic bonds.

One of the features of the Intrinsic Gravitational (IG) field of the helical structures from which particles are built is the ability to create electrical charge. BSM analysis unveils the physical meaning of the electrical charge as modulation of CL nodes by internal RL structures of the helical structures from which the elementary particles are built. In such aspect the energy of the electrical charge could be regarded as a part of IG energy of the particle in CL space environment. In a near filed range the proximity field of the charge particle possesses a spatial configuration, while in a far field range it appears as a point charge. The analysis of the vibrational motion of two atoms connected in molecule by electronic bonds allows to identify some quantum mechanical features. The vibration causes spatial modulation of the near electrical field created by the protons participating in the electronic bond. The mechanism responsible for this modulation is a quantum quasishrink effect discussed in Chapter 2. This effect is a result of slight change of the resonance frequency of EQ CL node in comparison to MQ CL node. The modulation features of CL space are analysed by using a total energy of the system that involves:

- the IG energy
- the energy of the electrical charge
- the kinetic energy of the involved particles
- the energy of the emitted or absorbed photon
- the vibrational energy

In analysis the IG field energy is presented as integration of IG forces from some initial value to infinity. Practically the integration does not go to infinity because in case of inverse cubic law the field strength falls vary fast with the distance.

$$E_{IG}(CP) = -2\int_{r_{ne}}^{\infty} \frac{G_o m_{po}^2}{r^3} dr = \frac{C_{IG}}{(L_q(1) + 0.6455L_p)^2} \qquad [(9.13)]$$

where: m_{po} is the Intrinsic mass of the proton, G_o is the intrinsic gravitational constant

$C_{IG} = G_o m_{po}^2$ - IG factor

Note: The factor 2 in front of the integral comes from the two arm branches (along abcd axes) of the CL space cell unit. They both are included in the *xyz* cell unit to which all the CL space parameters are referenced. All equations using C_{IG} factor in the following analysis confirms the need of factor 2.

The vibrational motion of the simple H2 molecule is analysed based on the total energy balance in which the energy of IG field is a major component. The total momentum energy balance at the equilibrium point is given by

$$\frac{C_{IG}}{q(L_q(1) + 06455L_p)^2} = \frac{2E_q}{q} + \frac{2E_K}{q} \text{ (eV)} \qquad [(9.18)]$$

where: $2E_q/q = 511$ KeV - is the energy of the two electrical charges (for two protons); $2E_K/q = 2 \times 13.6$ eV - is the kinetic energy of the two electrons.

The analysis unveils the vibrational states and one metastable state of H_2 ortho-I molecule. The obtained expression for the vibrational levels

of this molecule with good for accuracy for their identification is:

$$E_\upsilon = \frac{C_{IG}}{qr^2} - \frac{2E_q}{q} - \frac{2E_K}{q} + E_X \qquad (9.23)$$

$$r = [[L_q(1)](1-\pi\alpha^4(\upsilon_m-\upsilon)^2)] + 0.6455L_p \qquad (9.23.a)$$

The photoelectron and optical spectrum are analysed and the corresponding transitions and vibrational levels are identified. The calculated vibrational levels are compared to those identified from the optical spectrum. The calculated vibrational curve fits quite well to these levels after adjusting a small offset level corresponding to E_X, whose value is 6.26 (eV). It is likely a constant from the integration in Eq. [(9.13)] that influences slightly only the vertical position of the vibrational curve. The influence of this parameter on CIG, however, is intrinsically small (beyond 5 significant digit), so for the number of tasks it could be omitted. Therefore, Eq. [(9.18)] allows determination one very useful parameter of IG field - the factor C_{IG}

$$C_{IG} = (2h\nu_c + h\nu_c\alpha^2)(L_q(1) + 0.6455L_p) \qquad [(9.17)]$$

$$C_{IG} = G_0 m_{n0}^2 = 5.2651\times10^{-33}$$

Fig. [9.24] shows simultaneously the vibrational energy levels E_ν, calculated by Eq. [(9.23)] and those estimated from the optical transitions E(0-ν'') and E(1-ν'') in UV spectrum (Lyman system) provided by I. Dabrowsky (1984). More details about identification of the transitions are given in §9.6 in Chapter 9 of BSM. The fractional error between calculated levels and experimental data is in a range of +/- 0.035%. While the vibrational curve is usually drawn as energy level towards internuclear distance, the step-like curve is an energy level towards a vibrational quantum number. The obtained value of energy difference between the smallest and largest vibrational number is 4.4834 eV, pretty close to the experimentally obtained value of 4.478 eV.

The analysis indicates that the total energy balance according to Eq. [(9.18)] is kept very accurate, despite the large IG energy. Therefore:

The emission or absorption of a photon is a result of comparatively small disturbance of the total energy balance.

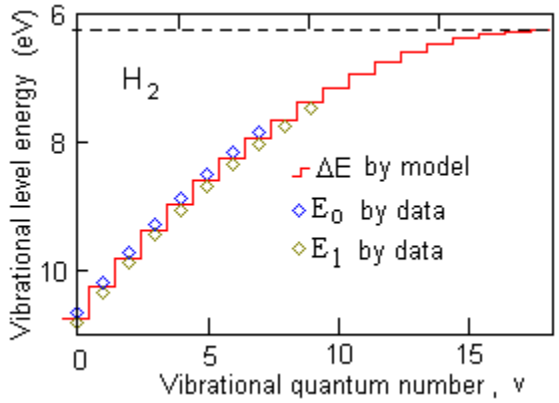

Fig. [9.24]. Energy levels E_ν, (eV) calculated by Eq. (9.23) towards the vibrational levels for H2 - ortho. The calculated levels are shown by step line, while the optical transitions corresponding to two different QM spins are shown by diamonds.

Similar analysis is provided also for D_2 molecule since it is a more typical building element in the atomic nuclei.

Note: The BSM model of vibrational motion works in highly nonlinear IG field, so it is quite different than the Quantum mechanical models. The obtained results are only for identification of the involved quantum effects and verification of the structure and spatial parameters of the particles: proton, neutron, electron. Therefore, despite the good match shown in Fig. [9.24] the calculated by Eq. [(9.23)] energy levels may differ from QM levels and especially for higher vibrational numbers.

Applying a total energy balance analysis for diatomic molecules an approximate expression for vibrational levels, ΔE of homonuclear molecules is obtained (BSM, Chapter 9, §9.15.2) It is approximate because the participated IG mass of the atomic nucleus is considered located in a point. In number of cases, however, the accuracy is enough for determination of the possible quantum orbit from the set of available quantum orbits. For this purpose a direct expression of internuclear distance of diatomic homonuclear molecule is derived from a conditions of total energy balance.

$$r_n(n,A,p) = (A-p)\sqrt{\frac{2\alpha C_{IG}}{pE_B(n)}} \qquad (9.56)$$

$$E_B(n) = \frac{C_{IG}}{[L_q(n) + 0.6455L_p]^2} - h\nu_c\left(2 - \frac{\alpha^2}{n}\right) \quad (9.56.a)$$

where: $E_B(n)$ - is a total energy involved in the bond connection of pair valence protons (deuterons), A - is the atomic mass for one atom in *daltons* (atomic mass units), p - is the number of protons involved in the bonding system (also per one atom), n - is the subharmonic quantum number of the quantum orbit, r_n - is the internuclear distance at the equilibrium vibrational point.

The quantum orbit could contained not only one but more quantum loops (see §7.4, Chapter 7 of BSM). In such case Eq. (9.56) and (9.56.a) obtains modifications, discussed in §9.15.3 of Chapter 9 of BSM.

The conditions defining the interatomic quantum orbits in molecules are different from those of atomic quantum orbits. In a latter case, the conditions determined the possible quantum orbit are determined by the proton dimensions, so they are stable. For interatomic quantum orbits in molecules, however, the defining conditions are influenced by the nuclear motion of involved atoms, in which the IG field interactions are involved. The IG forces are able to modulate the spatial configuration of the proximity E-field of the protons involved in the electronic bond. As a result, the vibrational quantum conditions occur at intrinsically small deviations from the internuclear distance. The actual vibrational range for H_2 ortho-I molecule is given by the expression

$$\delta r = 2\pi\alpha^4\upsilon_m^2 L_q(1) \quad (9.26)$$

For the identified maximum vibrational number $\upsilon_m = 18$, the range of vibrations is only $\delta r = 7.866\times10^{-16}$ (m) while the estimated internuclear distance is 2.23E-10 (m).

8. Method for determination the possible configurations of diatomic molecules

The possible configuration of diatomic molecules could be unveiled by simultaneous application of the following methods:

(a) a drawing method: using the spatial configuration of the nucleus and selected possible orbit from the quantum orbit set

(b) a theoretical calculation of the internuclear distance by Eq. (9).

(c) calculation of low number energy levels and comparing the results with transitions of identified spectral bands from the optical and photoelectron spectra (Note: The expression [(9.34)] is based on point IG masses and may not be accurate for diatomic molecules with a large Z number of atoms).

The intrinsically small change of the internuclear distance of vibrating within one band molecule, mentioned in the previous paragraph, facilitates the task for identification of the possible configuration of a simple molecule. Applying Eq. [(9.34)] for diatomic molecules in which Z>4, it is found that a quantum orbit of $L_q(1)$ is not possible due to the restrictions imposed by the finite size of the atomic nuclei. This additionally facilitates the task for identification of the possible states.

Fig. [9.42] shows the photoelectron spectra of O_2 molecule. They likely correspond to different internuclear distances.

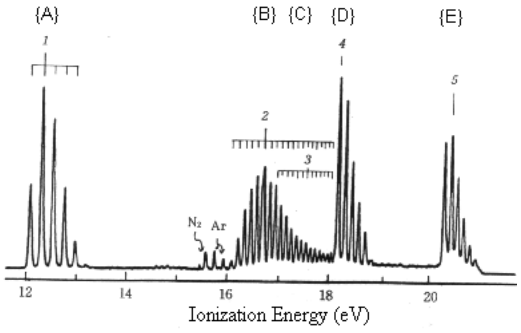

Fig. [9.42]. PE spectrum of O_2 molecule excited by He I radiation (Turner et all., courtesy of K. Kimura et al., (1981)). The capital letters in brackets is a notation used by BSM.

Table 9.6 shows the calculated internuclear distances for different quantum orbits L_q, using Eq. [(9.55)] (first raw) and the estimated distances by the drawing method (second raw).

Calculated by Eq. (9.55) values for r_n for O_2 states. The values are given in Angstroms (A). **Table 9.6**

r_n (A)	$L_q(2)$ (1 bond)	$L_q(2)$ (2 bonds)	$L_q(2x)$ (2 bonds)	$L_q(3)$ (2 bonds)
by Eq. (9)	2.57 A	1.698 A		1.219 A
by drawing	2 A	1.7 A	1.74 A	1.25 A
possible state	{B}or {C}	{D}	{E}	{A}

The bottom raw of Table 9.6 provides the possible states of O_2 molecule obtained by the two methods and their probable correspondence to the states of the photoionization spectrum shown in Fig. [9.42].

Some of the possible configurations the O_2 molecule, corresponding to different states are shown in Figures [9.43], [9.44] and [9.45].

9. Examples of possible configurations of some molecules

Note: In most of the following drawings the protons and neutrons in the central polar section of the atomic nucleus are only shown.

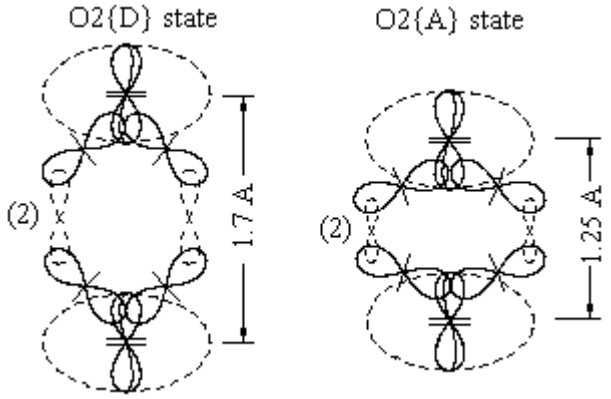

Fig. [9.43] Possible configurations of O_2(D) and O_2(A). {D} and {A} are states of O_2 according BSM model. The orbital planes of electrons do not lie in the drawing plane, but they are shown in this way for drawing simplification. The number in a bracket indicates the subharmonic number of the quantum orbit.

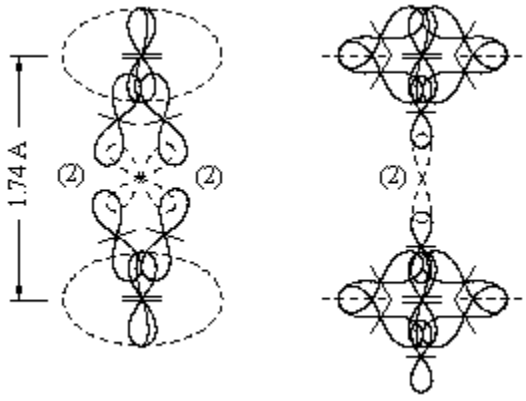

Fig. [9.45] A possible configuration of O_2 molecule in {E} state

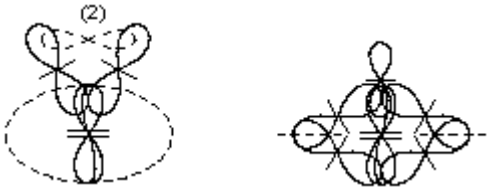

Fig. [9.53] Two views of the probable configuration of oxygen atom in Airglow state responsible for line emissions at 5577 A and 6300 A.

.

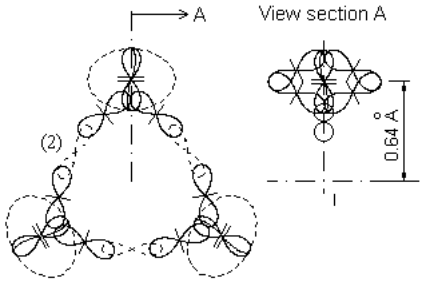

Fig. [9.53.A]
Ozone molecule with second subharmonic bonding orbits Every one of the three bonding orbits contains two electrons with opposite Quantum Mechanical spins

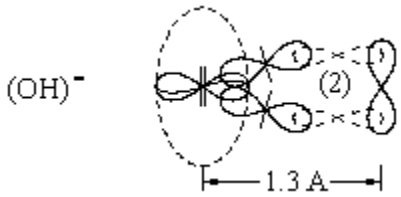

Fig. [9.54] Configuration of $(OH)^-$ ion. Every electronic bond orbit contains two electrons with opposite QM spins, so the molecule is symmetrical (the planes of bonding orbits are at 90 deg, in respect to the protons equivalent planes)

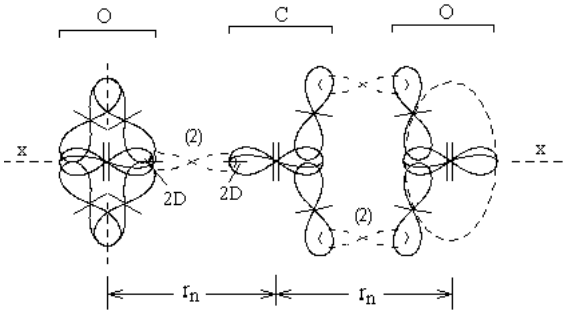

Fig. 9.56 One view of CO_2 molecule. The CO2 molecule possesses rotational symmetry about the polar axis due to the 90 deg rotational symmetry of C atom. If rotating 90 deg around zz axis the view of the left side will change with the view of the right side.

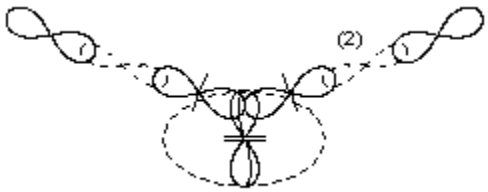

Fig. [9.59] Water molecule

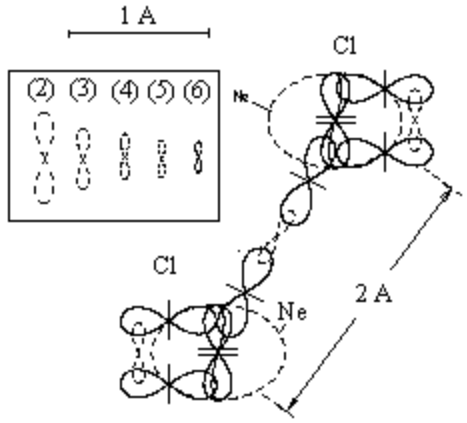

Fig. 9.7 Cl_2 molecule. The dashed oval is the envelope of Ne nucleus. A set of the possible quantum orbits is shown in the square box, where the number in bracket indicates the subharmonic number of electron quantum velocity. The experimental value of internuclear distance between Cl atoms is 1.98 A.

10. Rotational component in vibrational rotational spectra of molecules

The electronic type of chemical bonds allows a vibrational type of motion of the involved nuclei. The vibrational levels obtained by Eq. [(9.23)] for H_2 and [(9.34] for diatomic molecules corresponds to the most energetic transitions of the optical spectrum for zero rotational states. The BSM analysis leads to a conclusion that **the rotational components in the vibrational rotational spectra, according to BSM, are likely result of shape distortion of the quantum electronic orbits.**

The possible types of the shape distortion are:

- a symmetrical distortion
- an asymmetrical distortion

The both types of distortion are shown respectively in Fig. [9.16], a. and b.

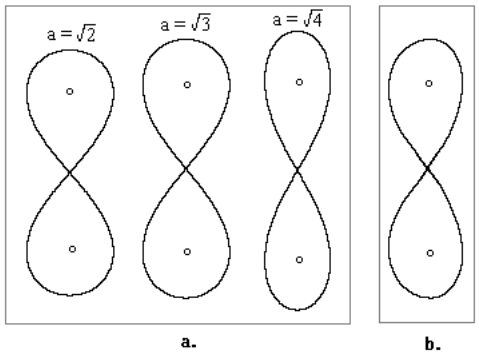

Fig. [9.16]

a. - symmetrical and b. - asymmetrical distortion of the bonding orbit

The vibrational motion of linear diatomic molecules involves symmetrical distortions of the bonding orbits. The effect of the distortion of the bonding orbit and its signature in the vibrational-rotational spectrum is illustrated by Fig. [9.17].

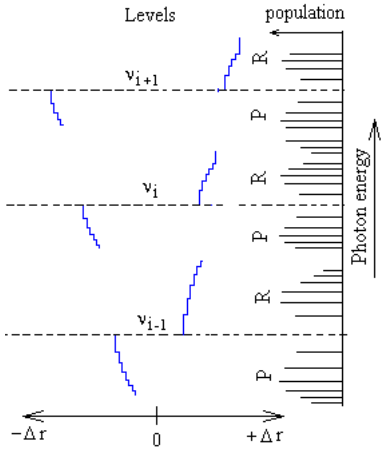

Fig. [9.17] Section of three consecutive levels of the vibrational ladder with fine structure levels from the bonding system frequency set. In the right side the corresponding optical spectrum from transition between these levels and the lowest level is shown.

For molecules with two binding orbits one of the bonds is a point of rotation at any moment (contributing to Q branch), while the other undergoes a symmetrical distortion (contributing to P and R branches) and they change alternatively.

The vibrational motion in bent molecules involves additional asymmetrical distortion of the binding quantum orbits. This effect contributes to folded P or R branches in some molecules with bent shape.

11. Structural and angular restrictions of the chemical bonds of electronic type

11.1. Restrictions from atomic nuclear configuration

The provided considerations in §5, §6 and §7 demonstrate that the structural and angular restrictions reduce significantly the degree of freedom of the atoms connected by electronic bonds. The same restrictions are also responsible for the molecular bending. These features are not apparent from the Quantum Mechanical models of the atoms.

The mentioned considerations are not valid for ionic bonds where the atoms are not connected by electronic bonds but by attractive forces between oppositely charged ions. The internuclear distances in ionic bonds are also larger and such molecules exhibit different physical properties. Consequently they are not able to possess vibrational motion in which the quantum orbits play important roles. For this reasons the ionic compounds don't have vibrational rotational spectra. Only separated ions are able to provide ionic line spectra.

The following conclusion is valid only for chemical compounds with electronic bonds, but not for compounds with ionic bonds.

- **The degrees of freedom of connected atoms in molecules by electronic bonds are reduced by structural restrictions and limited angular freedom of the valence protons. This restrictions are defined by the nuclear configurations of the involved atoms.**

11.2. Restrictions imposed by the nuclear configurations of the involved atoms

If not taking into account the existing one or more He nuclei (with their polar electrons) in the nucleus of anyone of the atoms, every single proton in the atom has own electron, connected to the free proton club (the club that is not polar attached). Some of these proton clubs, however, are GBclp or EB bonded in pairs. For EB bonded protons the two electrons with opposite QM spin circulate in a common orbit whose plane is almost parallel to the polar atomic axis. For GBclp bonded protons the two electrons with opposite spin circulate in a common orbit whose plane is almost perpendicular to the polar axis. In both cases, the common quantum orbit passes through the clubs of the protons. The orbital trajectory is well defined by the proximity E-field of the involved protons. The positions of GBclp protons are strongly fixed, while the EB protons are weakly fixed by the quantum orbits. Any fixed orbit may not lye in a plane but it is quite close to a fixed equivalent orbital plane that gets a proper symmetrical position in respect to the polar nuclear axis. From above mentioned consideration it is evident that the quantum orbits connected to BGps, GBclp and EB type of bonds have fixed orientation of their equivalent planes. These fixed positions are much stronger held in comparison to the orbital plane positions of the chemical bonds.

Table 4 provides the number of different type proton bonds in the nuclei of some elements and the total electrons with commonly aligned equivalent orbital planes (where: N_e - is the number of electrons with aligned equivalent orbital planes)

Table 4.

Atom	GBclp	EB	N_e
C	0	0	2
N	0	1	2
O	2	0	6
P	4	1	10
S	4	2	10
Cl	4	3	10
Ca	8	0	18
Fe	8	0	18
Cu	8	4	18

In the analysis provided in Chapter 8 and 9 of BSM it is found that two of the external shell protons of the oxygen atom are GBclp bonded. The signature indicating such type of bonding appears in the first ionization potential trend as a function of Z-number and also in the photoionization potential of the oxygen (known as autoionization feature). The nuclear structure of Oxygen is illustrated in Fig. 7.

In the right part of the drawing, the common positions of the fixed electron orbits are shown as viewed from the polar axis. The projections patterns of the two polar orbit electrons (1s electrons according to QM model) are shown by different colours. Their similar patterns exhibit angular ro-

tation around the polar axis due to the nuclear twisting of the atomic nucleus. This feature, valid for all atoms, is a result of the proton twisting. The GBclp bonded protons (deuterons) are shown in the plane of drawing while the valence protons (deuterons) are closely aligned to a perpendicular plane, but shown at oblique angles for a drawing simplification purpose.

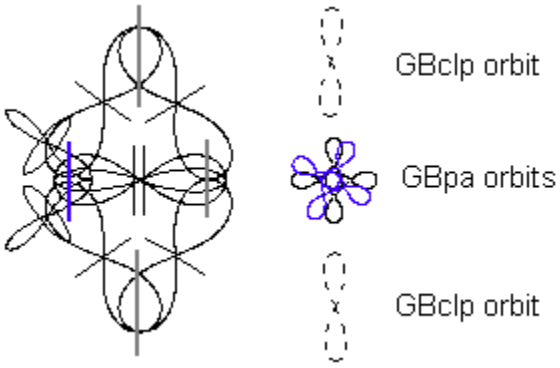

Fig. 7 Nuclear structure of the Oxygen atom. The two valence type protons in the left side of the nucleus are in fact in a plane perpendicular to the drawing

The stability of such nuclear configuration with two GBclp pairs is a result of the nuclear symmetry in which the two polar electrons (from 1s shell) have strong influence. This configuration provides much larger angular freedom of the two valence protons that may explain the large chemical activity of the Oxygen atom.

12. Validation of the structural features of BSM atomic models by the organic and biomolecules with known structure and atomic composition.

12.1. General considerations

The 3D structures and atomic compositions of many biomolecules now are well known. In such structures, the individual atoms are identified as nodes with known coordinates. The angular coordinates of their chemical bonds are also known. This information is sufficient in order to replace the nodes in the 3D structure of any large molecule with the physical models of the atoms according to BSM concept. If the BSM models are correct, their spatial configuration and angular bond restrictions should match the 3D structure of the biomolecules. Once the BSM models are validated and corrected if necessary, the complex biomolecules and any macromolecule with known shape could be studied from a new point of view. The application of the BSM models, for example, allows identification of the positions of all orbits. This includes the nuclear and the chemical bonds electronic orbits. Then the conditions for possible interactions, modifications and energy transfer could be analysed at atomic level. The carbon atom is one of the most abundant elements in the organic and biomolecules. The left part of Fig 8. shows the 3D structures of the carbon, while the right part shows the possible quantum orbits in the same scale. They are denoted by their subharmonic number (defined by the quantum velocity of the electron)

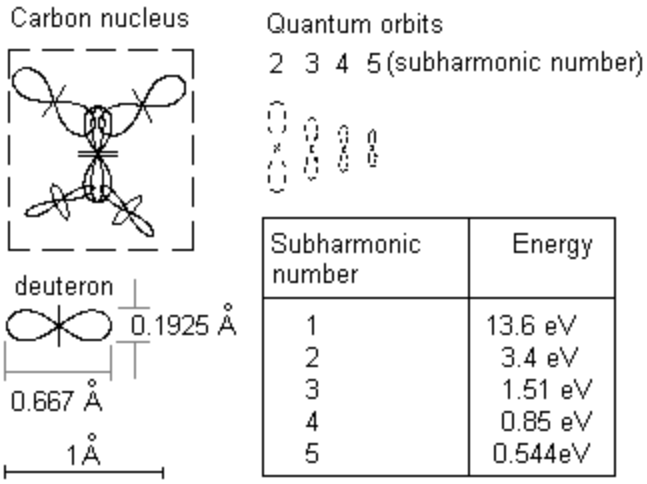

Subharmonic number	Energy
1	13.6 eV
2	3.4 eV
3	1.51 eV
4	0.85 eV
5	0.544eV

Fig. 8. Nuclear structure of carbon atom

12.2. Ring atomic structures in organic molecules.

Most of the organic molecules contain ring atomic structures. The molecule of benzene could be considered as a simple example of a ring structure. The biomolecules usually possess a large number of ring atomic structures. Fig. 9. shows the 3D molecular structure of aspirin where the ring structure of 6 carbon atoms is similar as in benzene. Fig. 10 shows the same structure of aspirin at atomic level by application of BSM atomic models.

.

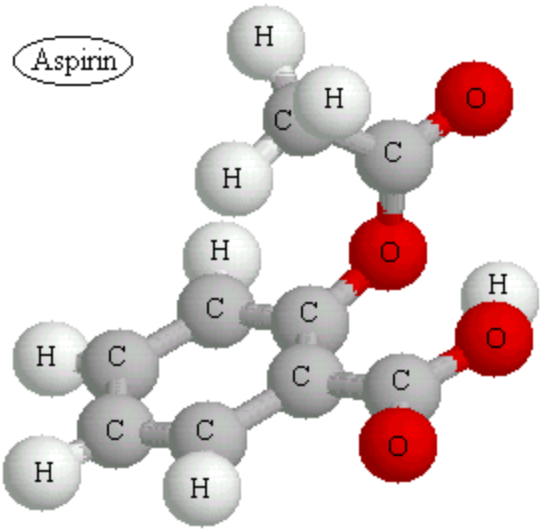

Fig. 9 Three dimensional structure of the molecule of aspirin (PDB file visualized by Chime software)

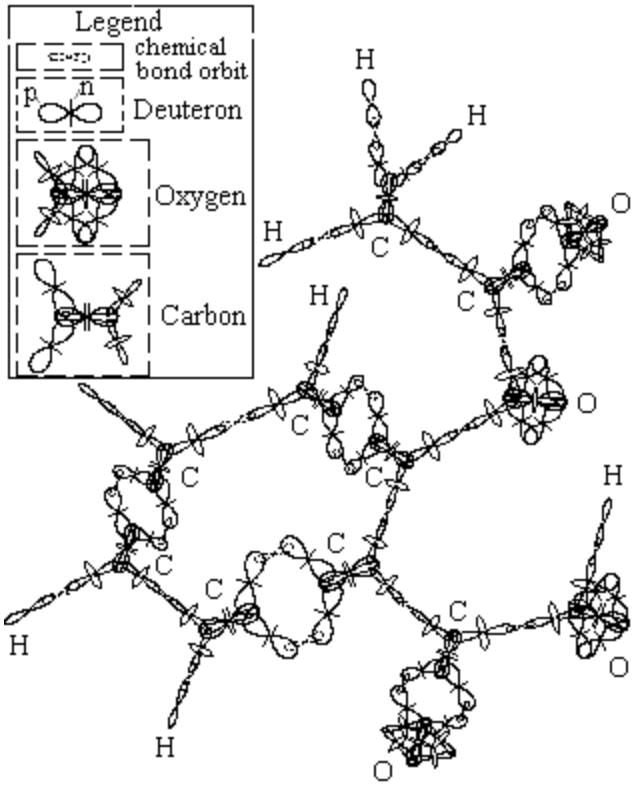

Fig. 10 Three dimensional structure of aspirin by BSM atomic models

The single atoms Deuteron, Oxygen and Carbon and the size of quantum orbit of second subharmonic are shown in the left upper corner. The valence protons (deuterons) of the oxygen atom are in fact in a plane perpendicular to the plane of EB bonded protons (deuterons) but they are shown with reduced dimensions in order to imitate an oblique angle in 3D view. The same is valid also for the valence protons of the carbon atom. In Fig. 9 the electronic orbits providing chemical bonds are only shown. For molecule with known 3D structure and composition the common positions of all electronic orbits with their equivalent orbital planes are identifiable. It is clearly apparent that the 3D structure of the molecule is defined by the following conditions:

(a) a finite size of the involved atomic nuclei

(b) an angular restricted freedom of valence protons

(c) a finite orbital trace length defined by the quantum conditions of the circulating electron

(d) orbital interactions

(e) a QM spin of the electron (the motion direction of the electron in respect to the proton twisting)

The QM mechanical models of atoms are mathematical models in which the features (c), (d), and (e) are directly involved, while the features (a) and (b) are indirectly involved by the selection of proper wavefunctions. In this process however some of the spatial and almost all angular restrictions are lost. Let emphasize now the difference between the suggested BSM models of atoms and molecules and the QM models:

- QM model: the electrons participating in chemical bonds are orbiting around both point-like nuclei, i. e. they are not localised

- BSM model: the electrons involved in the chemical bonds are localised

-QM model: the chemical bond lengths are estimated from the electron microscopy assuming the planetary atomic model in which the larger electron concentrations are centred around the poinlike nucleus

- BSM model: the chemical bond length may need re-estimation, because the orbits of the chemical bond electrons do not encircle the bound atomic nuclei.

- BSM model: the length of single C-C bond may vary only by the subharmonic number of quantum orbit, while the length in a double C=C bond is additionally dependent of the angular positions of the valence protons.

12.3 Some abundant atomic structures in biomolecules.

Ring structures are very abundant in many biomolecules and they are very often arranged in particular order along their chain. DNA and proteins contain large number of ring structures.

Fig.11 shows the spatial arrangement of ring atomic structures in a portion of β–type DNA. The positions of some (O+4C) rings from the deoxyribose molecule that is involved in the helical backbone strands of DNA are pointed by arrows.

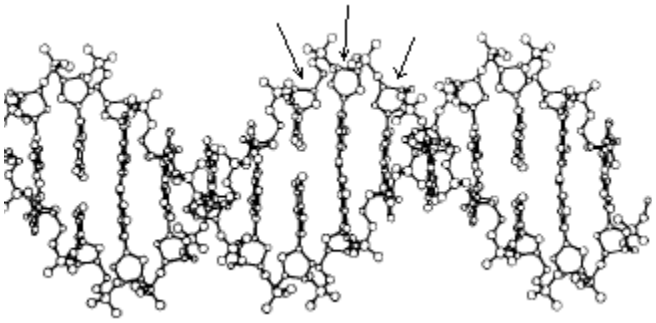

Fig. 11 Part of DNA structure with indicated positions of some of (O+5C) atomic rings

Fig. 12 shows the ring atomic structure (O+4C) from the DNA strand. The valence deuterons involved in the ring structure practically have some small twisting, but the quantum orbit of single valence bond also could be twisted. This feature gives some freedom for formation of ring structures of different atoms. The rotational freedom of the single valence bonds, however, may be accompanied by some stiffness that increases with the degree of the orbital twisting. Some of the atoms of the ring structure are also connected to other external atoms. All this considerations provide explanation why the ring structure (O+5C) connected to the DNA strand is not flat but curved.

The BSM atomic models unveil one important feature of the ring structure. The quantum orbits are localised in a ring. Therefore, it is likely possible the ring structure to be able to hold energy as a rotating excited state. This is reasonable if taking into account the spin-orbital interaction existing in atoms (discussed in Chapter 8). Then this could be a kind of energy storage mechanism. This issue is discussed in BSM_Application_3.

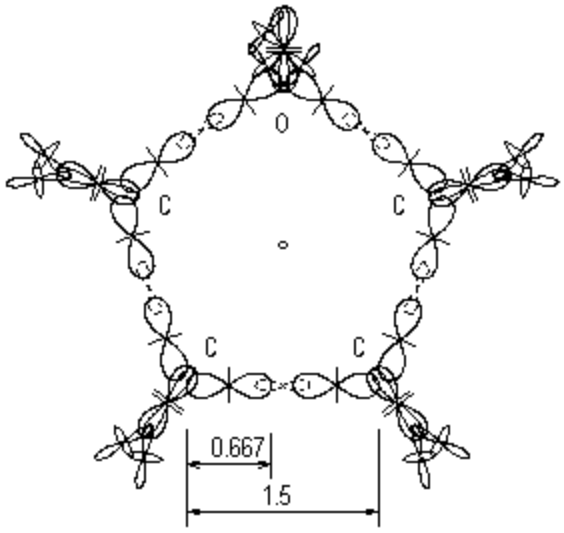

Fig. 12 Ring atomic structure from the deoxyribose molecule involved in DNA strand

12.4 Weak hydrogen bonds

It is known that a weak hydrogen bond is possible between two atoms, one of which does not possess a free valence. The bond connection is a result of orbital interactions. In such aspects the hydrogen bonds connecting the purines to pyramidines in DNA molecule are of two types: <N-H...O> and <N-H...N>, where the single valence electronic bond is denoted by "-" and the H-bond is denoted by "...". The BSM concept allows finding of the possible orbital orientation for such type of bond. This is illustrated by Fig. 13.

In a hydrogen bond of type N-H...O the plane of electronic orbit of hydrogen appears almost parallel to the commonly oriented nuclear orbits of oxygen atom in which six electrons are involved (see Table 4 and Fig. 7). In a hydrogen bond of type N-H...N the plane of electronic orbit of hydrogen is almost parallel to the equivalent planes of the two polar orbits of N in which two electrons are involved. It is evident that the hydrogen bond is characterized by the following features:

- the connection is a result of common orbital orientation
- the H-bond requires critical range of distance
- the H-bond allows a large rotational freedom

This three features allows the DNA molecule to possess excellent folding properties.

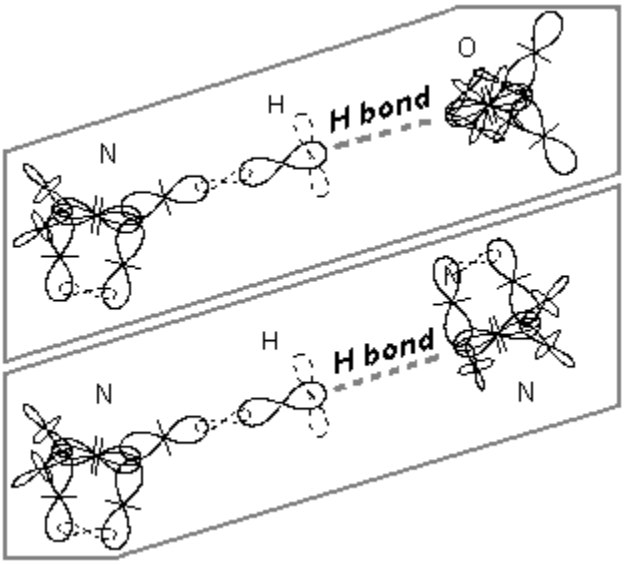

Fig. 13. Two types of hydrogen bonds

13. BSM atomic models and nanotechnology.

Fig. 14 shows a sheet of the unfolded cylindrical wall with identified valence of the chemical bonds, so that the four valences of all carbon atoms (excluding the edge atoms) are connected.

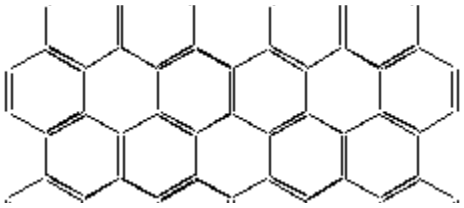

Fig. 14

Let considering the hexagonal ring as a unit structure of the sheet. Then the sheet is comprised of two types of ring structures:

- ring structure of I-st type (containing only single valence bonds)
- ring structures of II-nd type (containing tree single valence bonds and three second valence bonds).

Fig. 15 provides an axonometric view of a sheet, corresponding to unfolded cylindrical part of single walled carbon nanotube. The rings of I-st type are clearly distinguishable from the rings of II-nd type. The protons, involved in the second valence bonds lie in a plane perpendicular to the sheet plane. In the same figure all quantum orbits providing chemical bonding are also shown.

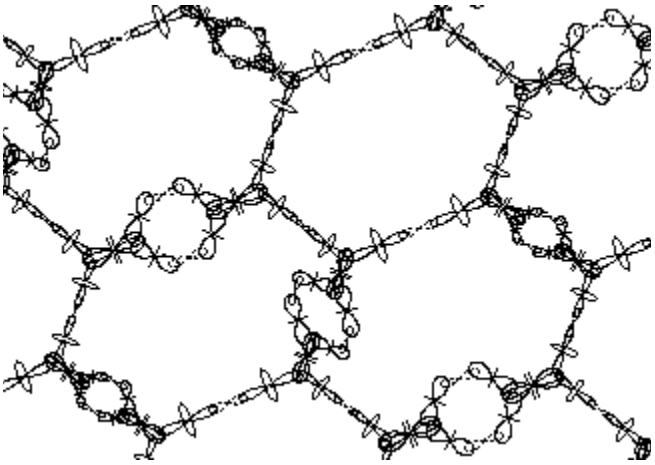

Fig. 15 Axonometric view of model of single wall sheet of carbon nanotube

Conclusions.

BSM theory is developed using a new approach and methodology with resurrected principle of objectivity, causality and logical understanding [18]. The reconsideration of space-time formulation gives a possibility for analysis of wide range of physical phenomena from a different point of view without need of the Heisenberg uncertainty principle. This allows unveiling deterministic relations in tough problems where the human logic was considered as failed. In such aspect the mysteries of the Quantum Mechanics, the General and the Special Relativity obtain logical explanations.

Between the major output results of the BSM theory are the unveiled structures of atomic nuclei and the physical models of the atoms. They can be reliably validated by existed data base about the atomic structure and compositions of organic and biomolecules. The physical models and understandable quantum interactions could be used for theoretical analysis of the energy processes in the biomolecules (see BSM _Application_3). Another potentially useful application is a “New vision about a controllable fusion reaction D+D->He with efficient energy yield” (BSM_Application_1).

The suggested BSM atomic models do not intend to undermine the Quantum Mechanical models of the atoms. The new vision is that they provide accurate calculations of QM interactions from energetic point of view, but they are not able to unveil the physical structures of the involved particles. Therefore they are mathematical models

only. From a point of view of BSM concept the ability of these models to provide accurate calculations of interaction energies is a result of intrinsic linearization feature in the unique conditions of self-sustainable CL grid, valid only for the energy scale. This linearization appears slightly disturbed only in boundary conditions of the ground state orbits (apparent in BSM model of Hydrogen, for example, presented in Chapter 7 of BSM). Its signature is the Lamb shift.

Applied in the field of cosmology the BSM analysis leads to a different concept about the evolution processes in the Universe, challenging the Big Bang model. A hypothesis of stationary universe with recycling galaxies is presented in Chapter 12 of BSM.

Finally the BSM theory may serve for building of successful unified field theory. The interdisciplinary analysis indicates that the relation matter-energy-gravitation is a fundamental one from which all known physical laws and postulates could be derived. The understanding of this relation may allow us to adopt the cold fusion energy and to control the gravitation.

References:

[1] T. H. Boyer, The Classical Vacuum, Scientific American, Aug. 1985, p.70-78.

[2] J. H. Black and A. Dalgarno, Interstellar H_2: The population of excited rotational states and the infrared response to ultraviolet radiation, Astrophysical Journal, **203**, 132-142 1976

[3] M. L. Gershteyn et al., Experimental evidence that the gravitational constant varies with orientation, http://arxiv.org/abs/physics/0202058

[4] I. Dabrowski, Can. J. Phys., **62**, 1639 (1984)

[5] A. Einstein, B. Podolsky and N. Rosenet al., Physical Review, **47**, 777-780 (1935)

[6] L. Ferrarese, D. Merrit, A fundamental relation between supermassive black holes and their host galaxies, arXiv: astro-ph/0006053 v. **29** Aug 2000

[7] S. Goldstein article on book of P. R. Holland, The Quantum theory in motion, Cambridge Univ. Press. Ney York, 1993, (Science, 263, 254-255 (1994))

[8] B. Haisch, A. Rueda and H. E. Puthoff, Inertia as a Zero-point filed lorenz force, Phys. Rev. A, **49**, 678 (1994). See also Science 263, 612 (1994)

[9] M. Ibison, H. E. Puthoff and S. R. Little. The Speed of Gravity Revisited, posted to LANL archives, http://xxx.lanl.gov/abs/physics/9910050

[10] K. Kimura et al., Handbook oh He I PE Spectra of Fundamental organic molecules, Japan Scientific Societies Press (1981)

[11] H. A. Lorentz, Nature, **113**, p. 608 (1924)

[12] P. J. Mohr and B. N. Taylor, CODATA recommended values of the fundamental physical constants: 1998, Rev. of Mod. Phys., vol.**72**, No 2, April, 351-495 (2000)

[13] S. Nagel, Physics in crisis, Physics Today, Sep 2002, 55-58

[14] H. E. Puthoff, Can the Vacuum be Engineered for Spaceflight applications, NASA Breakthrough Propulsion Physics, conference at Lewis Res. Center, (1977)

[15] D. F. Roscoe, An analysis of 900 optical rotation curves: Dark matter in a corner?, Phahama - journal of physics, Indian Academy of Sciences, Vol. **53**, No 6 Dec 1999, p. 1033-1037

[16] S. Sarg, “Basic Structures of Matter”, thesis, (2001), http://www.helical-structures.org
also in:
http://collection.nlc-bnc.ca/amicus/index-e.html
(AMICUS No. 27105955)

[17] S. Sarg, Atlas of Atomic Nuclear Structures (2001)
http://www.helical-structures.org
also in:
http://collection.nlc-bnc.ca/amicus/index-e.html
(AMICUS No. 27106037)

[18] S. Sarg, New approach for building of unified theory about the Universe and some results, http://lanl.arxiv.org/abs/physics/0205052 (2002)

[19] S. Sarg, New vision about a controllable fusion reaction D+D->He with efficient energy yield, http://www.helical-structures.org/Applications
also in: http://collection.nlc-bnc.ca/amicus/index-e.html
(AMICUS No. 27276360)

[20] M. Wales, Quantum Theory; Alternative Perspectives, Shields Books, www.fervor.demon.co.uk